Momentum-space Argonne V18 interaction

S. Veerasamy and W. N. Polyzou
Department of Physics and Astronomy, The University of Iowa, Iowa City, Iowa 52242, USA
(Received 14 January 2011; revised manuscript received 2 June 2011; published 8 September 2011)

This paper gives a momentum-space representation of the Argonne V18 potential as an expansion in products of spin-isospin operators with scalar coefficient functions of the momentum transfer. Two representations of the scalar coefficient functions for the strong part of the interaction are given. One is as an expansion in an orthonormal basis of rational functions and the other as an expansion in Chebyshev polynomials on different intervals. Both provide practical and efficient representations for computing the momentum-space potential that do not require integration or interpolation. Programs based on both expansions are available as supplementary material. Analytic expressions are given for the scalar coefficient functions of the Fourier transform of the electromagnetic part of the Argonne V18. A simple method for computing the partial-wave projections of these interactions from the operator expressions is also given.

DOI: 10.1103/PhysRevC.84.034003 PACS number(s): 21.45.Bc, 21.30.Cb

I. INTRODUCTION

The Argonne V18 potential [1] is one of a number of nucleon-nucleon interactions [1–3] that provide a quantitative description of experimental two-body observables below the pion-production threshold. It is distinguished from the other realistic interactions because it is expressed as an operator expansion with local configuration-space coefficient functions. This representation has advantages when used in variational Monte Carlo calculations. On the other hand, there are a number of calculations that require a realistic interaction that are more naturally performed in momentum space. These include some Faddeev calculations, relativistic few-body calculations, and calculations involving electromagnetic probes. In the momentum representation the variable conjugate to the relative coordinate is the momentum transfer. In calculations, both momenta appear, which requires either an interpolation or a separate Fourier transform for each pair of momenta. Fourier transforms of the V18 potential have been used in some applications [4]. The purpose of this paper is to provide useful, tested, and reproducible analytic approximations of the Fourier transform of the Argonne V18 potential for use in momentum-space calculations. The analytic forms allow for a direct calculation of the momentum-space interaction for any pair of initial and final momenta. In keeping with the traditional Argonne form, the momentum-space potential is given as a linear combination of products of spin-isospin operators with scalar functions of the momentum transfer. The resulting momentum-space potential has 24 terms. The additional six operators appear because the Fourier transform of the terms involving the operators $\mathbf{L}^2 V_i(r)$ and $(\mathbf{L}\cdot\mathbf{S})^2 V_i(r)$ each become a sum of two different momentum-space operators with different coefficient functions. In this work the Fourier transform is given for the strong part of the Argonne V18 potential, without the electromagnetic terms. This part of the potential must be treated numerically. The electromagnetic terms have analytic Fourier transforms, which are discussed in Appendix C. The partial-wave projection of the momentum-space potential is discussed in Appendix B. It is constructed from the operator expressions by integrating over the angle between the initial and final momentum vectors, however, unlike the configuration-space partial-wave projection, the integrals involve both the operator and the scalar coefficient functions.

The Argonne V18 potential has the form

$$V = \sum_{n=1}^{18} V_n(r) O_n \tag{1.1}$$

where $V_n(r)$ are rotationally-invariant coefficient functions of the relative coordinate of the nucleons and the O_n are the eighteen spin-isospin operators given in Table I. In this table T_{12} is the isotensor operator $T_{12} := 3\tau_{1z}\tau_{2z} - \boldsymbol{\tau}_1\cdot\boldsymbol{\tau}_2$. While the isospin operators, $\boldsymbol{\tau}_i$, factor out of the Fourier transforms, the operators L^2, $\mathbf{L}\cdot\mathbf{S}$, $(\mathbf{L}\cdot\mathbf{S})^2$, and the tensor operator S_{12} contribute to the Fourier transform.

The Fourier transform of this potential can be expressed as a linear combination of 24 momentum-space operators with scalar coefficient functions of the momentum transfer. There are 24 operators because the $\mathbf{L}\cdot\mathbf{L}$ and $(\mathbf{L}\cdot\mathbf{S})^2$ operators have two distinct contributions in momentum space. In Appendix A it is shown that the potential matrix element $\langle\mathbf{k}'|V|\mathbf{k}\rangle$, with $\mathbf{q} := \mathbf{k}' - \mathbf{k}$, has the following five types of contributions:

(i) $\mathbf{I}$

$$\frac{1}{(2\pi)^3}\int e^{-i(\mathbf{k}'-\mathbf{k})\cdot\mathbf{r}} V_j(r)\mathbf{I}d\mathbf{r} = \mathbf{I}\frac{1}{2\pi^2}\int_0^\infty j_0(qr)V_j(r)r^2dr. \tag{1.2}$$

(ii) $\mathbf{L}\cdot\mathbf{S}$

$$\frac{1}{(2\pi)^3}\int e^{-i\mathbf{k}'\cdot\mathbf{r}} V_j(r)\mathbf{L}\cdot\mathbf{S}e^{i\mathbf{k}\cdot\mathbf{r}}d\mathbf{r} = i(\mathbf{k}\times\mathbf{k}')\cdot\mathbf{S}\frac{1}{2\pi^2 q}\int_0^\infty j_1(qr)V_j(r)r^3dr. \tag{1.3}$$

TABLE I. Argonne V18 spin-isospin operators in coordinate space.

Term	Spin-isospin operator in r space
O_1	$\mathbf{I}$
O_2	$(\boldsymbol{\tau}_1 \cdot \boldsymbol{\tau}_2)$
O_3	$(\boldsymbol{\sigma}_1 \cdot \boldsymbol{\sigma}_2)$,
O_4	$(\boldsymbol{\sigma}_1 \cdot \boldsymbol{\sigma}_2)(\boldsymbol{\tau}_1 \cdot \boldsymbol{\tau}_2)$
O_5	$S_{12} = 3(\boldsymbol{\sigma}_1 \cdot \hat{\mathbf{r}})(\boldsymbol{\sigma}_2 \cdot \hat{\mathbf{r}}) - \boldsymbol{\sigma}_1 \cdot \boldsymbol{\sigma}_2$
O_6	$S_{12}(\boldsymbol{\tau}_1 \cdot \boldsymbol{\tau}_2)$,
O_7	$(\mathbf{L} \cdot \mathbf{S})$
O_8	$(\mathbf{L} \cdot \mathbf{S})(\boldsymbol{\tau}_1 \cdot \boldsymbol{\tau}_2)$
O_9	$(\mathbf{L} \cdot \mathbf{L})$
O_{10}	$(\mathbf{L} \cdot \mathbf{L})(\boldsymbol{\tau}_1 \cdot \boldsymbol{\tau}_2)$
O_{11}	$(\mathbf{L} \cdot \mathbf{L})(\boldsymbol{\sigma}_1 \cdot \boldsymbol{\sigma}_2)$
O_{12}	$(\mathbf{L} \cdot \mathbf{L})(\boldsymbol{\sigma}_1 \cdot \boldsymbol{\sigma}_2)(\boldsymbol{\tau}_1 \cdot \boldsymbol{\tau}_2)$
O_{13}	$(\mathbf{L} \cdot \mathbf{S})^2$
O_{14}	$(\mathbf{L} \cdot \mathbf{S})^2(\boldsymbol{\tau}_1 \cdot \boldsymbol{\tau}_2)$
O_{15}	$T_{12} = (3\tau_{1z}\tau_{2z} - \boldsymbol{\tau} \cdot \boldsymbol{\tau})$
O_{16}	$(\boldsymbol{\sigma}_1 \cdot \boldsymbol{\sigma}_2)T_{12}$
O_{17}	$S_{12}T_{12}$
O_{18}	$(\tau_{1z} + \tau_{2z})$

(iii) $\mathbf{L} \cdot \mathbf{L}$

$$\frac{1}{(2\pi)^3}\int e^{-i\mathbf{k}'\cdot\mathbf{r}} V_j(r)\mathbf{L}\cdot\mathbf{L} e^{i\mathbf{k}\cdot\mathbf{r}} d\mathbf{r}$$
$$= -(\mathbf{k}'\times\mathbf{k})\cdot(\mathbf{k}'\times\mathbf{k})\frac{1}{2\pi^2 q^2}\int_0^\infty j_2(qr)V_j(r)r^4 dr$$
$$+ 2(\mathbf{k}'\cdot\mathbf{k})\frac{1}{2\pi^2 q}\int_0^\infty j_1(qr)V_j(r)r^3 dr. \quad (1.4)$$

(iv) $(\mathbf{L} \cdot \mathbf{S})^2$

$$\frac{1}{(2\pi)^3}\int e^{-i\mathbf{k}'\cdot\mathbf{r}} V_j(r)(\mathbf{L}\cdot\mathbf{S})^2 e^{i\mathbf{k}\cdot\mathbf{r}} d\mathbf{r}$$
$$= -(\mathbf{S}\cdot(\mathbf{k}\times\mathbf{k}'))^2\frac{1}{2\pi^2 q^2}\int_0^\infty j_2(qr)V_j(r)r^4 dr$$
$$+ (\mathbf{k}'\times\mathbf{S})\cdot(\mathbf{k}\times\mathbf{S})\frac{1}{2\pi^2 q}\int_0^\infty j_1(qr)V_j(r)r^3 dr. \quad (1.5)$$

(v) $S_{12} = 3(\hat{\mathbf{r}}\cdot\boldsymbol{\sigma}_1)(\hat{\mathbf{r}}\cdot\boldsymbol{\sigma}_2) - \boldsymbol{\sigma}_1\cdot\boldsymbol{\sigma}_2$

$$\frac{1}{(2\pi)^3}\int e^{-i\mathbf{k}'\cdot\mathbf{r}} V(r)\left[3(\hat{\mathbf{r}}\cdot\boldsymbol{\sigma}_1)(\hat{\mathbf{r}}\cdot\boldsymbol{\sigma}_2) - \boldsymbol{\sigma}_1\cdot\boldsymbol{\sigma}_2\right] e^{i\mathbf{k}\cdot\mathbf{r}} d\mathbf{r}$$
$$= -\left[3(\mathbf{q}\cdot\boldsymbol{\sigma}_1)(\mathbf{q}\cdot\boldsymbol{\sigma}_2) - q^2\boldsymbol{\sigma}_1\cdot\boldsymbol{\sigma}_2\right]\frac{1}{2\pi^2 q^2}$$
$$\times\int_0^\infty j_2(qr)V(r)r^2 dr. \quad (1.6)$$

These expressions are used to represent the momentum-space interaction as a sum of scalar functions of $q := |\mathbf{q}|$ multiplied by spin-isospin operators. These scalar coefficient functions of the momentum transfer that multiply the spin-isospin operators have the form of one of the integrals listed in Table II: where $V_m(r)$ is the mth potential in the expansion [Eq. (1.1)] and $\tilde{V}_{ma}(q)$ and $\tilde{V}_{mb}(q)$ are the two different functions that appear in Eqs. (1.4) and (1.5). These functions have finite limits as $q \to 0$ in spite of the $1/q^l$ coefficients since the Bessel function $j_l(qr)$ vanishes like q^l as $q \to 0$. The strong interaction contribution to the 24 scalar coefficients listed in Table II are numerically computed. The computational methods are discussed in Sec. 3. Programs that compute these scalar coefficients are available as supplementary material to the electronic version of this paper. Quantities, like the binding energies in the test calculations, exhibit small sensitivities (in the sixth significant figure) to the precision of input constants. In the supplementary programs these constants are taken from the original V18 potential.

The supplementary programs are c source codes. For a given input q they produce four arrays corresponding to the four types of integrals in Table II. The index m on the array corresponds to the m values (without the a or b) in Table II. When one of the integrals in Table II has no contribution for a particular m value the entry is set to zero. Both programs calculate the same quantities using the two different methods described in this paper.

The electromagnetic contribution to each of these operators can be represented in terms of known special functions. These contributions are important for precise low-energy calculations and can be added to the strong interaction coefficient functions when they are needed. The analytic expressions for the electromagnetic terms are given in Appendix B.

The resulting momentum-space potential has an operator expansion of the form

$$\langle\mathbf{k}'|V|\mathbf{k}\rangle = \sum_{m\in S}\tilde{V}_m(q)\tilde{O}_m, \quad (1.7)$$

where $S = \{1, 2, 3, 4, 5, 6, 7, 8, 9a, 9b, 10a, 10b, 11a, 11b, 12a, 12b, 13a, 13b, 14a, 14b, 15, 16, 17, 18\}$ and the 24 operators $\tilde{O}_m$ are given in Table III.

The Argonne V18 potential in momentum space has the dimension (MeV fm^3). Dividing by $\hbar c$ in (MeV-fermi) can be used to convert the momentum-space potential to a consistent set of units, [(fm)^2].

II. NUMERICAL FOURIER BESSEL TRANSFORMS

This section summarizes an accurate numerical computation of the integrals in Table II. These computations are used to test the accuracy of the approximations discussed in the next section.

Because the configuration-space potential falls off asymptotically like $e^{-m_\pi r}$, the radial integrals are evaluated with a finite cutoff at 20 fm. The Fourier-Bessel transforms are evaluated for momentum transfers $q < 100$ fm^{-1}. With these cutoffs the maximum value of $x := qr$ that can appear in the argument of the spherical Bessel functions in the integrals in Table II. is $x_{\max} = 2000$. To evaluate these integrals the zeros of the spherical Bessel functions $j_0(x)$, $j_1(x)$, and $j_2(x)$ for $0 \leqslant x \leqslant 2000$ are computed for each fixed value of q. For each value of q the integrals are expressed as sums of integrals between successive zeros of the spherical Bessel function that appear in the integral. If q is such that qr is never a zero of $j_l(qr)$ for $0 < r < 20$ fm then the integral over r is performed using a 100-point Gauss-Legendre quadrature on the interval

TABLE II. Momentum-space scalar coefficient functions.

Scalar coefficient function	Dim	Indices
$\tilde{V}_m(q) := \frac{1}{2\pi^2}\int_0^\infty j_0(qr)V_m(r)r^2dr$	MeV fm^3	$m \in \{1, 2, 3, 4, 15, 16, 18\}$
$\tilde{V}_m(q) := \frac{1}{2\pi^2 q}\int_0^\infty j_1(qr)V_m(r)r^3dr$	MeV fm^5	$m \in \{7, 8, 9b, 10b, 11b, 12b, 13b, 14b\}$
$\tilde{V}_m(q) := \frac{1}{2\pi^2 q^2}\int_0^\infty j_2(qr)V_m(r)r^4dr$	MeV fm^7	$m \in \{9a, 10a, 11a, 12a, 13a, 14a\}$
$\tilde{V}_m(q) := \frac{1}{2\pi^2 q^2}\int_0^\infty j_2(qr)V_m(r)r^2dr$	MeV fm^5	$m \in \{5, 6, 17\}$

$[0, 20\,\text{fm}]$. If q is such that qr has zeros of $j_l(qr)$ for $0 < r < 20$ fm, then the integrals between zeros $[qr_i, qr_{i+1}]$ are computed using 20 Gauss-Legendre points when $r_{i+1} \leqslant 5$ fm, 40 Gauss-Legendre points when $5\,\text{fm} < r_{i+1} \leqslant 10\,\text{fm}$ and 80 Gauss-Legendre points when $10\,\text{fm} < r_{i+1} \leqslant 20\,\text{fm}$. For further details see Ref. [5].

III. APPROXIMATIONS

This section discusses two approximations of the potential functions $\tilde{V}_m(q)$ in Table II by expansions in known elementary functions. The first method approximates these potential functions by linear combinations of Chebyshev polynomials on three distinct intervals of momenta, for momenta up to 100 fm^{-1}. The second approach approximates these potential functions by a finite linear combination of orthonormal functions of the momentum transfer that have analytic Fourier-Bessel transforms. The configuration-space basis functions are associated Laguerre polynomials multiplied by decaying exponentials. These functions have analytic Fourier transforms that are rational functions of the momentum transfer [8]. In both approaches the coefficients of the expansion function are stored. The basis functions at any point can be generated efficiently by recursion and the potentials can be expressed as a finite linear combination of the basis functions. Both methods lead to efficient and accurate approximations to the momentum-space potential.

Figures 1 and 2 show the potential functions for the central and tensor parts $[V_1(q)$ and $V_5(q)]$ of the interaction to illustrate the structure of typical potentials.

A. Chebyshev expansions

This section discusses the Chebyshev basis. The functions $\tilde{V}_m(q)$ are replaced by a Chebyshev polynomial approximation on the interval $q \in [a, b]$ using [6]

$$\tilde{V}_m(q) \approx c_0/2 + \sum_{n=1}^{100} c_n T_n\left(-\frac{a+b}{b-a} + \frac{2}{b-a}q\right) \tag{3.1}$$

where

$$T_n(x) = \cos[n\cos^{-1}(x)] \tag{3.2}$$

are Chebyshev polynomials and the coefficients c_n are computed using a Clenshaw-Curtiss quadrature [6]

$$c_n = \frac{2}{N}\left\{\frac{1}{2}\tilde{V}_m(b) + \sum_{j=1}^{N-1}\tilde{V}_m\left[\frac{a+b}{2} + \frac{b-a}{2}\cos(\pi j/N)\right] \times \cos(nj\pi/N) + (-)^n\frac{1}{2}\tilde{V}_m(a)\right\} \tag{3.3}$$

with $N = 101$. The functions $\tilde{V}_m(q)$ are evaluated at the quadrature points $q_j := \frac{a+b}{2} + \frac{b-a}{2}\cos(\pi j/N)$ using the methods discussed above. This is repeated for q in each of three intervals, $[a, b] = [0, 10], [10, 50], [50, 100]$ and the 101 expansion coefficients associated with each of these three intervals are stored. The Chebyshev polynomials are computed using the recurrence relations

$$T_{n+1}(x) = 2xT_n(x) - T_{n-1}(x), \quad T_0(x) = 1, \quad T_1(x) = x. \tag{3.4}$$

For q larger than 100 fm^{-1} $\tilde{V}_m(q)$ is approximated by 0.

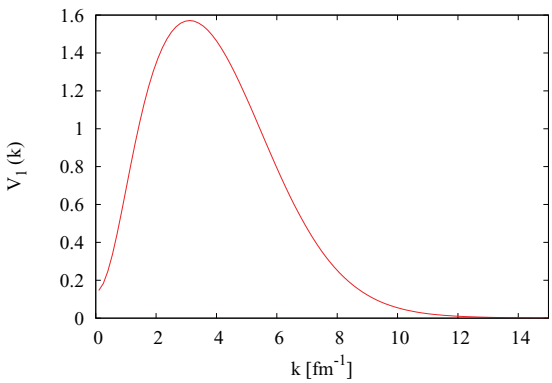

FIG. 1. (Color online) $\Delta V_1(k)$.

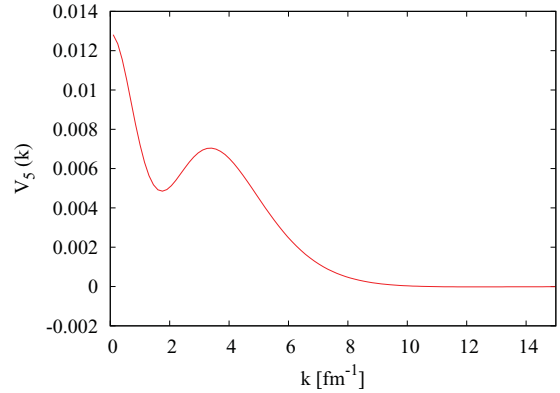

FIG. 2. (Color online) $V_5(k)$.

TABLE III. Argonne V18 momentum-space spin-isospin operators.

Term	Spin-isospin operator
$\tilde{O}_1$	$\mathbf{I}$
$\tilde{O}_2$	$(\boldsymbol{\tau}_1 \cdot \boldsymbol{\tau}_2)$
$\tilde{O}_3$	$(\boldsymbol{\sigma}_1 \cdot \boldsymbol{\sigma}_2)$
$\tilde{O}_4$	$(\boldsymbol{\sigma}_1 \cdot \boldsymbol{\sigma}_2)(\boldsymbol{\tau}_1 \cdot \boldsymbol{\tau}_2)$
$\tilde{O}_5$	$-\left(3(\mathbf{q} \cdot \boldsymbol{\sigma}_1)(\mathbf{q} \cdot \boldsymbol{\sigma}_2) - q^2 \boldsymbol{\sigma}_1 \cdot \boldsymbol{\sigma}_2\right)$
$\tilde{O}_6$	$-\left(3(\mathbf{q} \cdot \boldsymbol{\sigma}_1)(\mathbf{q} \cdot \boldsymbol{\sigma}_2) - q^2 \boldsymbol{\sigma}_1 \cdot \boldsymbol{\sigma}_2\right)(\boldsymbol{\tau}_1 \cdot \boldsymbol{\tau}_2)$
$\tilde{O}_7$	$i(\mathbf{k} \times \mathbf{k}') \cdot \mathbf{S}$
$\tilde{O}_8$	$i(\mathbf{k} \times \mathbf{k}') \cdot \mathbf{S}(\boldsymbol{\tau}_1 \cdot \boldsymbol{\tau}_2)$
$\tilde{O}_{9a}$	$-(\mathbf{k}' \times \mathbf{k}) \cdot (\mathbf{k}' \times \mathbf{k})$
$\tilde{O}_{9b}$	$2(\mathbf{k}' \cdot \mathbf{k})$
$\tilde{O}_{10a}$	$-(\mathbf{k}' \times \mathbf{k}) \cdot (\mathbf{k}' \times \mathbf{k})(\boldsymbol{\tau}_1 \cdot \boldsymbol{\tau}_2)$
$\tilde{O}_{10b}$	$2(\mathbf{k}' \cdot \mathbf{k})(\boldsymbol{\tau}_1 \cdot \boldsymbol{\tau}_2)$
$\tilde{O}_{11a}$	$-(\mathbf{k}' \times \mathbf{k}) \cdot (\mathbf{k}' \times \mathbf{k})(\boldsymbol{\sigma}_1 \cdot \boldsymbol{\sigma}_2)$
$\tilde{O}_{11b}$	$2(\mathbf{k}' \cdot \mathbf{k})(\boldsymbol{\sigma}_1 \cdot \boldsymbol{\sigma}_2)$
$\tilde{O}_{12a}$	$-(\mathbf{k}' \times \mathbf{k}) \cdot (\mathbf{k}' \times \mathbf{k})(\boldsymbol{\sigma}_1 \cdot \boldsymbol{\sigma}_2)(\boldsymbol{\tau}_1 \cdot \boldsymbol{\tau}_2)$
$\tilde{O}_{12b}$	$2(\mathbf{k}' \cdot \mathbf{k})(\boldsymbol{\sigma}_1 \cdot \boldsymbol{\sigma}_2)(\boldsymbol{\tau}_1 \cdot \boldsymbol{\tau}_2)$
$\tilde{O}_{13a}$	$-(\mathbf{S} \cdot (\mathbf{k} \times \mathbf{k}'))^2$
$\tilde{O}_{13b}$	$(\mathbf{k}' \times \mathbf{S}) \cdot (\mathbf{k} \times \mathbf{S})$
$\tilde{O}_{14a}$	$-(\mathbf{S} \cdot (\mathbf{k} \times \mathbf{k}'))^2(\boldsymbol{\tau}_1 \cdot \boldsymbol{\tau}_2)$
$\tilde{O}_{14b}$	$(\mathbf{k}' \times \mathbf{S}) \cdot (\mathbf{k} \times \mathbf{S})(\boldsymbol{\tau}_1 \cdot \boldsymbol{\tau}_2)$
$\tilde{O}_{15}$	T_{12}
$\tilde{O}_{16}$	$(\boldsymbol{\sigma}_1 \cdot \boldsymbol{\sigma}_2)T_{12}$
$\tilde{O}_{17}$	$-\left(3(\mathbf{q} \cdot \boldsymbol{\sigma}_1)(\mathbf{q} \cdot \boldsymbol{\sigma}_2) - q^2 \boldsymbol{\sigma}_1 \cdot \boldsymbol{\sigma}_2\right) T_{12}$
$\tilde{O}_{18}$	$(\tau_{1z} + \tau_{2z})$.

TABLE IV. Values of scalar coefficients at 1 fm^{-1}.

n	RFExp	CExp	NFT
1	6.789973×10^{-1}	6.789977×10^{-1}	6.789977×10^{-1}
2	-4.019392×10^{-1}	-4.019392×10^{-1}	-4.019392×10^{-1}
3	-1.692090×10^{-1}	-1.692090×10^{-1}	-1.692090×10^{-1}
4	2.358519×10^{-1}	2.356704×10^{-1}	2.356705×10^{-1}
5	7.216739×10^{-3}	7.218217×10^{-3}	7.218217×10^{-3}
6	2.857732×10^{-1}	2.860471×10^{-1}	2.860467×10^{-1}
7	-5.511547×10^{-1}	-5.511547×10^{-1}	-5.511547×10^{-1}
8	-1.678888×10^{-1}	-1.678888×10^{-1}	-1.678888×10^{-1}
9	1.741415×10^{-1}	1.741415×10^{-1}	1.741415×10^{-1}
10	-3.272988×10^{-2}	-3.272987×10^{-2}	-3.272987×10^{-2}
11	1.999136×10^{-2}	1.999136×10^{-2}	1.999136×10^{-2}
12	-7.414060×10^{-3}	-7.414060×10^{-3}	-7.414060×10^{-3}
13	9.084422×10^{-2}	9.084424×10^{-2}	9.084424×10^{-2}
14	1.245017×10^{-1}	1.245017×10^{-1}	1.245017×10^{-1}
15	1.122388×10^{-2}	1.122389×10^{-2}	1.122389×10^{-2}
16	-1.214926×10^{-2}	-1.216021×10^{-2}	-1.216031×10^{-2}
17	2.403290×10^{-3}	2.420818×10^{-3}	2.420818×10^{-3}
18	6.124964×10^{-3}	6.124964×10^{-3}	6.124964×10^{-3}
19	1.304278×10^{-2}	1.304274×10^{-2}	1.304274×10^{-2}
20	-1.702409×10^{-2}	-1.702401×10^{-2}	-1.702401×10^{-2}
21	-7.227244×10^{-3}	-7.227256×10^{-3}	-7.227256×10^{-3}
22	-7.849686×10^{-3}	-7.849707×10^{-3}	-7.849707×10^{-3}
23	4.518193×10^{-2}	4.518262×10^{-2}	4.518262×10^{-2}
24	3.980251×10^{-2}	3.980269×10^{-2}	3.980269×10^{-2}

For the potentials $\tilde{V}_4(q)$, $\tilde{V}_6(q)$, and $\tilde{V}_{17}(q)$ it was necessary to add additional Chebyshev expansions intervals between zero and ten fm^{-1}. For $\tilde{V}_4(q)$ 21 polynomials were used on [0, .2] fm^{-1}, 31 polynomials were used on [.2, .5] fm^{-1}, 41 polynomials were used on [.5, 2.0] fm^{-1} and 71 polynomials were used on [2.0, 10.0] fm^{-1}. For $\tilde{V}_6(q)$ 31 polynomials were used on [0, .5] fm^{-1}, 41 polynomials were used on [.5, 2.0] fm^{-1} and 41 polynomials were used on [2.0, 10.0] fm^{-1}. Similarly for $\tilde{V}_{17}(q)$ 31 polynomials were used on [0, 1.0] fm^{-1}, 51 polynomials were used on [1.0, 5.0] fm^{-1} and 51 polynomials were used on [5.0, 10.0] fm^{-1}.

This method provides an accurate and efficient representation for computing a momentum space V18 interaction. One of the supplementary programs (argonne_chebyshev.c [7]) uses this method to compute the 24 coefficient functions in Table II.

B. Rational basis functions

While the method of the previous section gives accurate results, a more straightforward approach is to represent the potential directly as an expansion in basis functions that have analytic Fourier transforms. In order to represent the potential, each of the scalar potentials $\tilde{V}_m(q)$, is approximated by an expansion in known basis functions. A method to compute both the expansion coefficients and a recursion formula to compute basis functions are given below.

The functions $V_m(r)$, $rV_m(r)$, and $r^2V_m(r)$ that appear in the integrands of the integrals in Table II are expanded using an orthonormal set of radial functions that have analytic Fourier-Bessel transforms [8]. These functions are associated Laguerre polynomials multiplied by decaying exponentials in configuration space. Their Fourier-Bessel transforms have power-law falloff in momentum space. In addition, they vanish at the origin in a manner that can be used to explicitly cancel the factors $1/q$ and $1/q^2$ that appear in the definitions of $\tilde{V}_m$ in Table II. Both sets of basis functions can be generated efficiently using recursion relations. The cancellation of the factors $1/q$ and $1/q^2$ can be directly incorporated into the recursion that generates the momentum-space basis functions so the final expression for the potential does not require a special treatment for q near 0.

The radial basis functions for different values of l are given below. The dimensionless parameter $x := \Lambda r$ is used in the basis functions, where Λ is a scale parameter that can be chosen to improve efficiency. The parametrization of the Argonne V18 interaction uses the value $\Lambda = 7(\text{fm})^{-1}$. The configuration-space basis functions are

$$\phi_{nl}(r) = \frac{1}{\sqrt{N_{nl}}} x^l L_n^{2l+2}(2x) e^{-x} \tag{3.5}$$

where

$$L_n^{\alpha} = \sum_{m=0}^{n} (-)^m \binom{n+\alpha}{n-m} \frac{x^m}{m!} \tag{3.6}$$

and the normalization coefficient is

$$N_{\text{nl}} = \Lambda^{-3} \left(\frac{1}{2}\right) \left(\frac{1}{2}\right)^{2l+3} \frac{\Gamma(n+\alpha+1)}{n!}. \tag{3.7}$$

TABLE V. Value of scalar coefficients at 5 fm^{-1}.

n	RFExp	CExp	NFT
1	1.160699×10^{0}	1.160699×10^{0}	1.160699×10^{0}
2	-1.360382×10^{-2}	-1.360382×10^{-2}	-1.360382×10^{-2}
3	-1.148807×10^{-1}	-1.148807×10^{-1}	-1.148807×10^{-1}
4	-1.065288×10^{-1}	-1.065203×10^{-1}	-1.065203×10^{-1}
5	4.489757×10^{-3}	4.489763×10^{-3}	4.489763×10^{-3}
6	4.405849×10^{-3}	4.405371×10^{-3}	4.405370×10^{-3}
7	-4.623736×10^{-2}	-4.623736×10^{-2}	-4.623736×10^{-2}
8	-1.871380×10^{-2}	-1.871380×10^{-2}	-1.871380×10^{-2}
9	2.471311×10^{-2}	2.471311×10^{-2}	2.471311×10^{-2}
10	1.480758×10^{-3}	1.480758×10^{-3}	1.480758×10^{-3}
11	6.027203×10^{-3}	6.027203×10^{-3}	6.027203×10^{-3}
12	1.465070×10^{-3}	1.465070×10^{-3}	1.465070×10^{-3}
13	5.222260×10^{-3}	5.222260×10^{-3}	5.222260×10^{-3}
14	8.233502×10^{-3}	8.233502×10^{-3}	8.233502×10^{-3}
15	4.828280×10^{-3}	4.828280×10^{-3}	4.828280×10^{-3}
16	-4.815794×10^{-3}	-4.815305×10^{-3}	-4.815305×10^{-3}
17	1.656921×10^{-6}	1.627533×10^{-6}	1.627533×10^{-6}
18	4.274306×10^{-4}	4.274306×10^{-4}	4.274306×10^{-4}
19	4.273833×10^{-3}	4.273832×10^{-3}	4.273832×10^{-3}
20	1.791462×10^{-4}	1.791461×10^{-4}	1.791461×10^{-4}
21	9.672551×10^{-4}	9.672550×10^{-4}	9.672550×10^{-4}
22	1.814761×10^{-4}	1.814761×10^{-4}	1.814761×10^{-4}
23	1.620319×10^{-3}	1.620318×10^{-3}	1.620318×10^{-3}
24	1.790086×10^{-3}	1.790085×10^{-3}	1.790085×10^{-3}

TABLE VI. Value of scalar coefficients at 15 fm^{-1}.

n	RFExp	CExp	NFT
1	9.321365×10^{-4}	9.321031×10^{-4}	9.321031×10^{-4}
2	4.123439×10^{-5}	4.123387×10^{-5}	4.123387×10^{-5}
3	-1.924812×10^{-5}	-1.924669×10^{-5}	-1.924669×10^{-5}
4	-6.648375×10^{-5}	-6.643904×10^{-5}	-6.643770×10^{-5}
5	-9.010902×10^{-6}	-9.010512×10^{-6}	-9.010512×10^{-6}
6	1.026393×10^{-5}	1.026324×10^{-5}	1.026323×10^{-5}
7	5.541260×10^{-6}	5.540856×10^{-6}	5.540856×10^{-6}
8	2.632043×10^{-6}	2.631901×10^{-6}	2.631901×10^{-6}
9	-1.962835×10^{-6}	-1.962585×10^{-6}	-1.962585×10^{-6}
10	-9.304609×10^{-7}	-9.304846×10^{-7}	-9.304846×10^{-7}
11	-6.015901×10^{-7}	-6.015363×10^{-7}	-6.015363×10^{-7}
12	-1.047669×10^{-7}	-1.047529×10^{-7}	-1.047529×10^{-7}
13	-4.725022×10^{-6}	-4.725152×10^{-6}	-4.725152×10^{-6}
14	-1.527634×10^{-6}	-1.527584×10^{-6}	-1.527584×10^{-6}
15	2.942747×10^{-6}	2.942623×10^{-6}	2.942623×10^{-6}
16	-2.895027×10^{-6}	-2.892432×10^{-6}	-2.892244×10^{-6}
17	$-2.865458 \times 10^{-10}$	$-3.049671 \times 10^{-10}$	$-3.061292 \times 10^{-10}$
18	9.986465×10^{-8}	9.985107×10^{-8}	9.985107×10^{-8}
19	-2.604487×10^{-7}	-2.604660×10^{-7}	-2.604660×10^{-7}
20	-6.335039×10^{-8}	-6.334951×10^{-8}	-6.334951×10^{-8}
21	-7.055132×10^{-8}	-7.055521×10^{-8}	-7.055521×10^{-8}
22	-1.454468×10^{-8}	-1.454569×10^{-8}	-1.454569×10^{-8}
23	-3.115148×10^{-7}	-3.115089×10^{-7}	-3.115089×10^{-7}
24	-1.394089×10^{-7}	-1.394129×10^{-7}	-1.394129×10^{-7}

These functions satisfy the orthogonality relations

$$\int_0^\infty \phi_{\rm nl}(r)\phi_{\rm ml}(r)r^2dr = \delta_{\rm mn}. \tag{3.8}$$

They have analytic Fourier-Bessel transforms given by

$$\tilde{\phi}_{\rm nl}(q) = \sqrt{\frac{2}{\pi}}\int_0^\infty j_l(qr)\phi_{\rm nl}(r)r^2dr. \tag{3.9}$$

For $y = q/\Lambda$ the $\tilde{\phi}_{\rm nl}(q)$ can be expressed in terms of Jacobi polynomials:

$$\tilde{\phi}_{\rm nl}(q) = \frac{1}{\sqrt{\tilde{N}_{\rm nl}}}\frac{y^l}{(y^2+1)^{l+2}}P_n^{l+\frac{3}{2},l+\frac{1}{2}}\left(\frac{y^2-1}{y^2+1}\right) \tag{3.10}$$

with normalization coefficient

$$\tilde{N}_{\rm nl} = \frac{\Lambda^3}{2(2n+2l+3)}\frac{\Gamma\left(n+l+\frac{5}{2}\right)\Gamma\left(n+l+\frac{3}{2}\right)}{n!\Gamma(n+2l+3)} \tag{3.11}$$

and

$$P_n^{(\alpha,\beta)}(x) = \frac{\Gamma(\alpha+n+1)}{n!\Gamma(\alpha+\beta+n+1)}\sum_{m=0}^{n}\binom{n}{m} \times \frac{\Gamma(\alpha+\beta+n+m+1)}{2^m\Gamma(\alpha+m+1)}(x-1)^m. \tag{3.12}$$

These functions satisfy the orthogonality relations

$$\int_0^\infty \tilde{\phi}_{\rm nl}(q)\tilde{\phi}_{\rm ml}(q)q^2dq = \delta_{\rm mn}. \tag{3.13}$$

These basis functions can be generated by using the recursion formulas for the associated Laguerre functions and Jacobi polynomials

$$(n+1)L_{n+1}^{\alpha}(x) = (2n+\alpha+1-x)L_{n+}^{\alpha}(x) - (n+\alpha)L_{n-1}^{\alpha}(x) \tag{3.14}$$

and

$$\begin{aligned}2(n+1)(n+\alpha+\beta+1)(2n+\alpha+\beta)P_{n+1}^{(\alpha,\beta)}(x) &= [(2n+\alpha+\beta+1)(\alpha^2-\beta^2)+x(2n+\alpha+\beta) \\ &\times(2n+\alpha+\beta+1)(2n+\alpha+\beta+2)]P_n^{(\alpha,\beta)}(x) \\ &-2(n+\alpha)(n+\beta)(2n+\alpha+\beta+2)P_{n-1}^{(\alpha,\beta)}(x).\end{aligned} \tag{3.15}$$

These recursion relations can be modified to incorporate the normalization constants [Eqs. (3.7) and (3.11)] directly into the recursion. The recursion for the normalized radial basis functions with ($x = \Lambda r$) is given by

$$\phi_{0l}(r) = \frac{1}{\sqrt{(2l+1)!}}\frac{1}{\sqrt{2^{2l+3}}}\Lambda^{3/2}x^l e^{-x} \tag{3.16}$$

$$\phi_{1l}(r) = \frac{2l+3-2x}{\sqrt{2l+3}}\phi_{0l}(r) \tag{3.17}$$

$$\phi_{\rm nl}(r) = \frac{2n+1+2l-2x}{\sqrt{n+1+2l}\sqrt{n}}\phi_{n-1,l}(r) - \sqrt{\frac{(n-1)(n+1+2l)}{n(n+2+2l)}}\phi_{n-2,l}(r). \tag{3.18}$$

Similarly, the normalized momentum-space basis functions with ($y = q/\Lambda$) are generated by the recursion

TABLE VII. Value of scalar coefficients at 25 fm^{-1}.

n	RFExp	CExp	NFT
1	-1.386301×10^{-5}	-1.383431×10^{-5}	-1.383431×10^{-5}
2	-6.108349×10^{-8}	-6.010007×10^{-8}	-6.010007×10^{-8}
3	8.598072×10^{-7}	8.595154×10^{-7}	8.595154×10^{-7}
4	1.014189×10^{-6}	1.003839×10^{-6}	1.003915×10^{-6}
5	-4.600082×10^{-7}	-4.599210×10^{-7}	-4.599210×10^{-7}
6	4.739733×10^{-7}	4.738710×10^{-7}	4.738711×10^{-7}
7	2.443040×10^{-8}	2.442088×10^{-8}	2.442088×10^{-8}
8	9.428095×10^{-9}	9.412965×10^{-9}	9.412965×10^{-9}
9	-1.534834×10^{-8}	-1.533919×10^{-8}	-1.533919×10^{-8}
10	3.457372×10^{-10}	3.607579×10^{-10}	3.607579×10^{-10}
11	-3.619628×10^{-9}	-3.613201×10^{-9}	-3.613201×10^{-9}
12	-1.005784×10^{-9}	-1.003137×10^{-9}	-1.003137×10^{-9}
13	4.666338×10^{-9}	4.709390×10^{-9}	4.709390×10^{-9}
14	-3.274714×10^{-9}	-3.270324×10^{-9}	-3.270324×10^{-9}
15	-5.425469×10^{-8}	-5.415686×10^{-8}	-5.415686×10^{-8}
16	5.452722×10^{-8}	5.398602×10^{-8}	5.399643×10^{-8}
17	$-2.888773 \times 10^{-12}$	$-4.263050 \times 10^{-12}$	$-4.213031 \times 10^{-12}$
18	-5.852151×10^{-9}	-5.841440×10^{-9}	-5.841440×10^{-9}
19	$-2.512190 \times 10^{-10}$	$-2.555613 \times 10^{-10}$	$-2.555613 \times 10^{-10}$
20	7.827015×10^{-12}	7.411785×10^{-12}	7.411785×10^{-12}
21	$-5.864134 \times 10^{-11}$	$-5.980761 \times 10^{-11}$	$-5.980761 \times 10^{-11}$
22	$-1.617550 \times 10^{-11}$	$-1.652711 \times 10^{-11}$	$-1.652711 \times 10^{-11}$
23	8.297311×10^{-11}	8.271942×10^{-11}	8.271943×10^{-11}
24	$-5.322500 \times 10^{-11}$	$-5.424546 \times 10^{-11}$	$-5.424546 \times 10^{-11}$

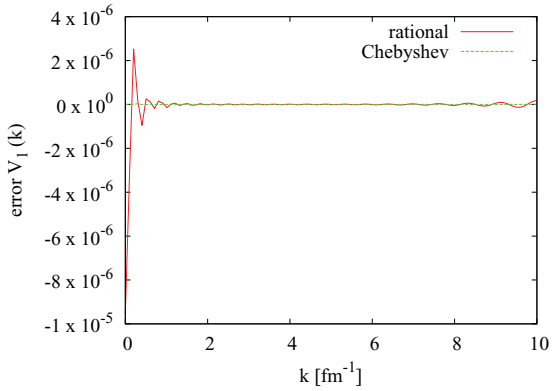

FIG. 3. (Color online) $\Delta V_{1\,\mathrm{rational}}(k)$, $\Delta V_{1\,\mathrm{Chebyshev}}(k)$.

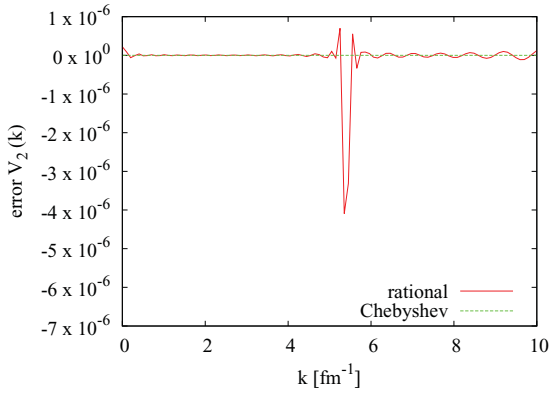

FIG. 4. (Color online) $\Delta V_{2\,\mathrm{rational}}(k)$, $\Delta V_{2\,\mathrm{Chebyshev}}(k)$.

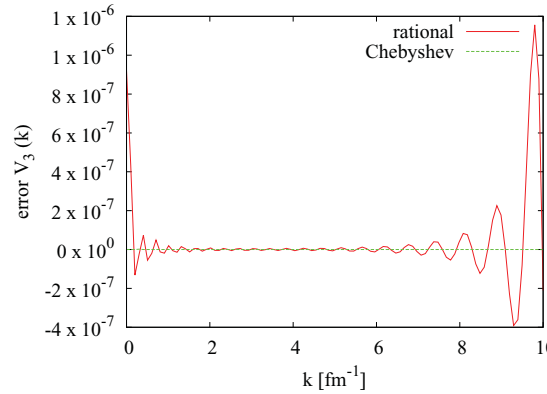

FIG. 5. (Color online) $\Delta V_{3\,\mathrm{rational}}(k)$, $\Delta V_{3\,\mathrm{Chebyshev}}(k)$.

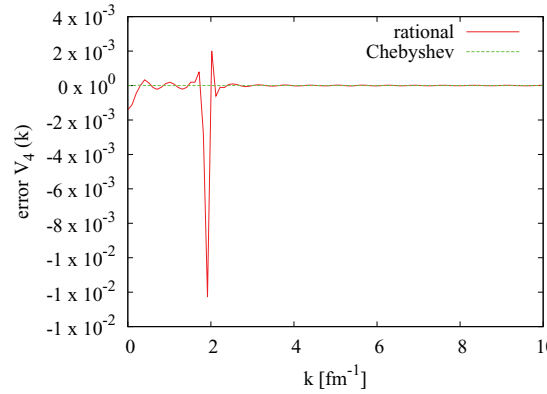

FIG. 6. (Color online) $\Delta V_{4\,\mathrm{rational}}(k)$, $\Delta V_{4\,\mathrm{Chebyshev}}(k)$.

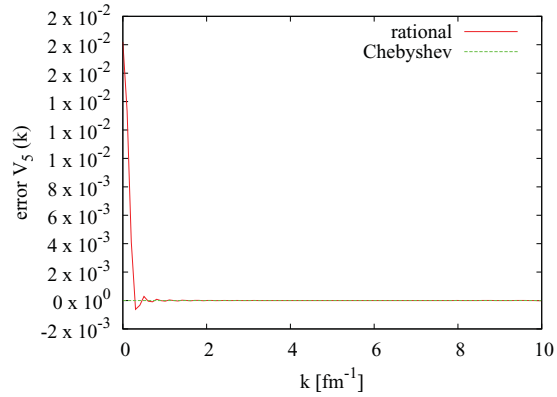

FIG. 7. (Color online) $\Delta V_{5\,\mathrm{rational}}(k)$, $\Delta V_{5\,\mathrm{Chebyshev}}(k)$.

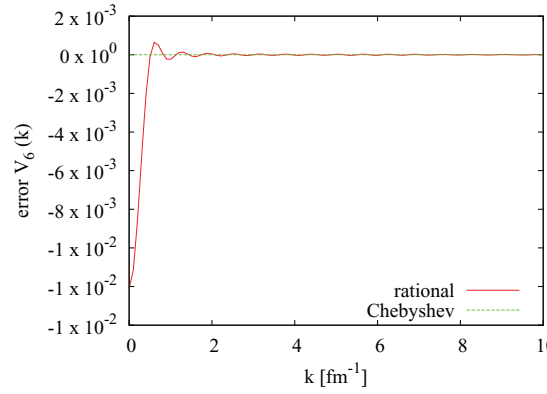

FIG. 8. (Color online) $\Delta V_{6\,\mathrm{rational}}(k)$, $\Delta V_{6\,\mathrm{Chebyshev}}(k)$.

$$\tilde{\phi}_{0l}(q) = \frac{1}{\sqrt{(2l+3)!}} \frac{1}{\sqrt{\Lambda^3}} \frac{1}{\sqrt{\frac{1}{2}\cdots\frac{2l+3}{2}}} \frac{1}{\sqrt{\frac{1}{2}\cdots\frac{2l+1}{2}}} y^l \frac{1}{(y^2+1)^{2l+2}} \tag{3.19}$$

$$\tilde{\phi}_{1l}(q) = \left(\frac{1}{2} + (l+2)\frac{y^2-1}{y^2+1}\right)\sqrt{\frac{2l+5}{\left(l+2+\frac{1}{2}\right)\left(l+1+\frac{1}{2}\right)}}\tilde{\phi}_{0l}(q) \tag{3.20}$$

$$\begin{aligned}\tilde{\phi}_{\mathrm{nl}}(q) = &\sqrt{\frac{(2n+2l+3)n(n+2l+2)}{(2n+2l+1)\left(n+l+\frac{3}{2}\right)\left(n+l+\frac{1}{2}\right)}} \\ &\times \frac{(2n+2l+1)(2l+2)(y^2+1)+(2n+2l+1)(2n+2l)(2n+2l+2)(y^2-1)}{2n(n+2l+2)(2n+2l)(y^2-1)}\tilde{\phi}_{n-1l}(q) \\ &-\sqrt{\frac{(2n+2l+3)(n-1)n(n+1+2l)(n+2l+2)}{(2n+2l-1)\left(n+l+\frac{3}{2}\right)\left(n+l+\frac{1}{2}\right)\left(n+l+\frac{1}{2}\right)\left(n+l-\frac{1}{2}\right)}} \times \frac{\left(n+l+\frac{1}{2}\right)\left(n+l-\frac{1}{2}\right)(2n+2l+2)}{(n)(n+2l+2)(2n+2l)}\tilde{\phi}_{n-1l}(q).\end{aligned} \tag{3.21}$$

Replacing $\tilde{\phi}_{0l}(q)$ in Eq. (3.19) by $\hat{\phi}_{0l}(q) := \tilde{\phi}_{0l}(q)/q^l$ given by

$$\hat{\phi}_{0l}(q) = \frac{1}{\sqrt{(2l+3)!}} \frac{1}{\sqrt{\Lambda^3}} \frac{1}{\sqrt{\frac{1}{2}\cdots\frac{2l+3}{2}}} \frac{1}{\sqrt{\frac{1}{2}\cdots\frac{2l+1}{2}}} \Lambda^{-l} \frac{1}{(y^2+1)^{2l+2}} \tag{3.22}$$

to start the recursion in Eqs. (3.20) and (3.21) generates $\hat{\phi}_{\mathrm{nl}}(q) := \tilde{\phi}_{\mathrm{nl}}(q)/q^l$, which are well-behaved as $q \to 0$. Seventy expansion coefficients are used to construct the momentum-space potential for each value

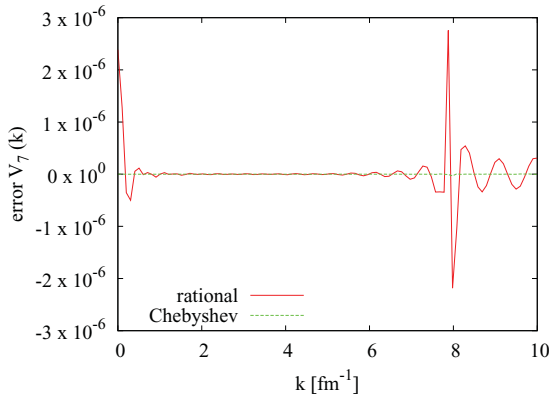

FIG. 9. (Color online) $\Delta V_{7\,\mathrm{rational}}(k)$, $\Delta V_{7\,\mathrm{Chebyshev}}(k)$.

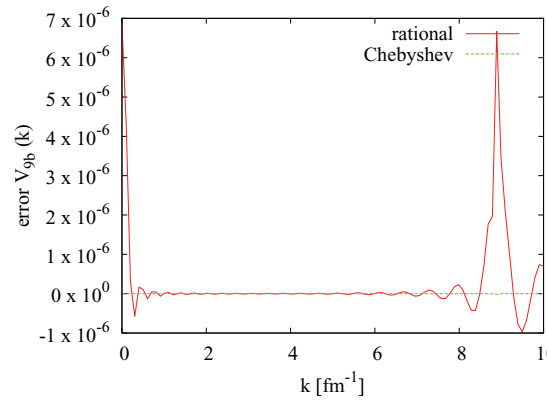

FIG. 11. (Color online) $\Delta V_{9b\,\mathrm{rational}}(k)$, $\Delta V_{9b\,\mathrm{Chebyshev}}(k)$.

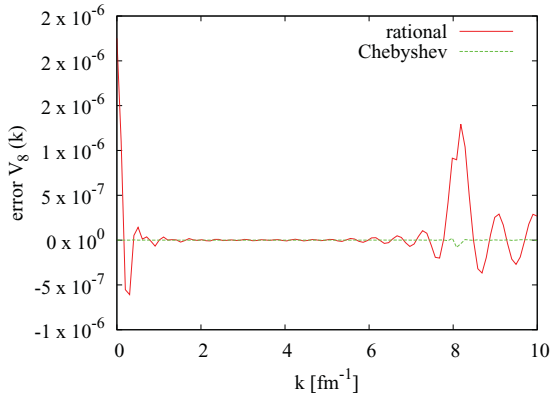

FIG. 10. (Color online) $\Delta V_{8\,\mathrm{rational}}(k)$, $\Delta V_{8\,\mathrm{Chebyshev}}(k)$.

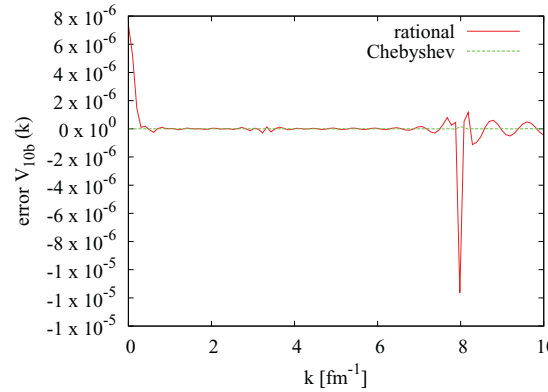

FIG. 12. (Color online) $\Delta V_{10b\,\mathrm{rational}}(k)$, $\Delta V_{10b\,\mathrm{Chebyshev}}(k)$.

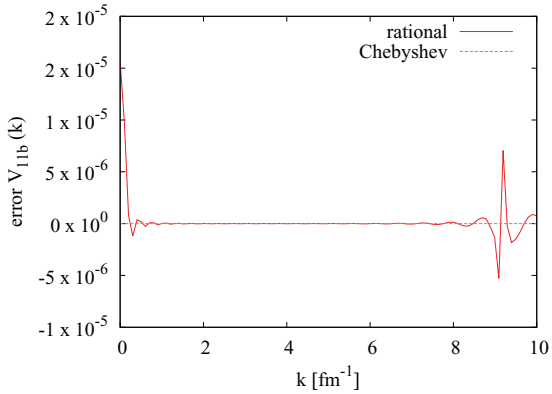

FIG. 13. (Color online) $\Delta V_{11b\,\mathrm{rational}}(k)$, $\Delta V_{11b\,\mathrm{Chebyshev}}(k)$.

of m

$$c_{\mathrm{nm}} = \frac{1}{2\pi^2}\int_0^\infty \phi_{n0}(r)V_m(r)r^2dr \times m \in \{1, 2, 3, 4, 15, 16, 18\} \quad (3.23)$$

$$c_{\mathrm{nm}} = \frac{1}{2\pi^2}\int_0^\infty \phi_{n1}(r)V_m(r)r^3dr \times m \in \{7, 8, 9b, 10b, 11b, 12b, 13b, 14b\} \quad (3.24)$$

$$c_{\mathrm{nm}} = \frac{1}{2\pi^2}\int_0^\infty \phi_{n2}(r)V_m(r)r^4dr \times m \in \{9a, 10a, 11a, 12a, 13a, 14a\} \quad (3.25)$$

$$c_{\mathrm{nm}} = \frac{1}{2\pi^2}\int_0^\infty \phi_{n2}(r)V_m(r)r^2dr \times m \in \{5, 6, 17\}. \quad (3.26)$$

The integrals are approximated using an 80 point Gauss-Legendre quadrature between 0 and 10 fm. The basis functions $\phi_{\mathrm{nl}}(r)$ are generated using Eqs. (3.16)–(3.18). The scale parameter in the recursion for $\phi_{\mathrm{nl}}(r)$ is taken as $\Lambda = 7$ fm^{-1}.

The 70x24 expansion coefficients c_{nm} are stored. The momentum-space potential functions are then given by

$$\tilde{V}_m(q) = \sum_{n=1}^{70} c_{\mathrm{nm}}\hat{\phi}_{\mathrm{nl}}(q) \quad (3.27)$$

where the reduced expansion functions $\hat{\phi}_{\mathrm{nl}}(q) := \tilde{\phi}_{\mathrm{nl}}(q)/q^l$ are generated recursively using Eqs. (3.20)–(3.22).

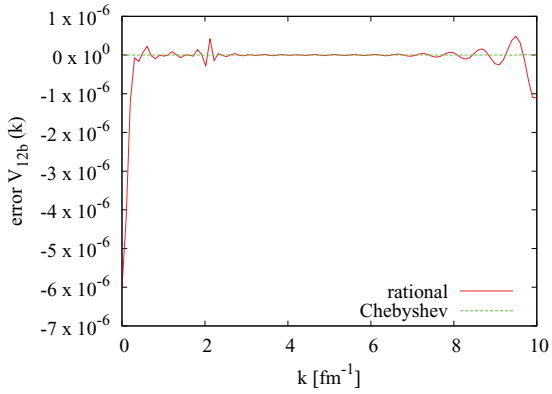

FIG. 14. (Color online) $\Delta V_{12b\,\mathrm{rational}}(k)$, $\Delta V_{12b\,\mathrm{Chebyshev}}(k)$.

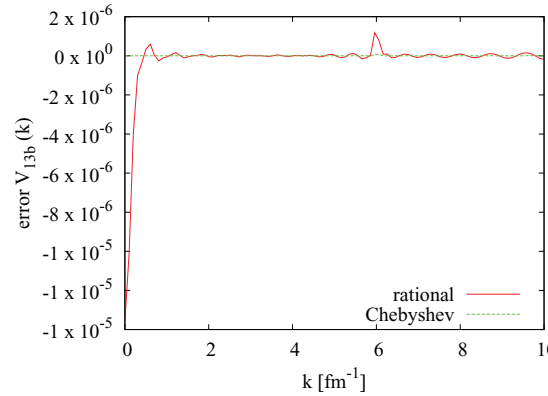

FIG. 15. (Color online) $\Delta V_{13b\,\mathrm{rational}}(k)$, $\Delta V_{13b\,\mathrm{Chebyshev}}(k)$.

The full momentum-space potential in operator form is given by

$$V = \sum_{m\in S} \tilde{V}_m(q)\tilde{O}_m \quad (3.28)$$

where $\tilde{O}_m$ are the 24 operators in Table III and $q = \sqrt{k^2 + k'^2 - 2\mathbf{k}'\cdot\mathbf{k}}$.

One of the supplementary programs (argonne_rational.c [9]) uses this method to compute the 24 coefficient functions in Table II.

IV. TESTS

Two tests are performed on the potentials. First, the momentum-space coefficient functions, $\tilde{V}_m(q)$, computed using the accurate numerical Fourier Bessel transforms, the Chebyshev expansion and the rational basis function expansion are compared. For the second test both representations of the potential are used to compute the deuteron binding energy and wave functions. These results are compared to a direct calculation of these quantities using the partial-wave expansion of the original configuration space potential.

The results of the first test are shown in Tables IV–VII, which list values of the Fourier-Bessel transforms of the 24 radial functions computed using these three different methods for momentum transfers of 1, 5, 15, and 25 fm^{-1}.

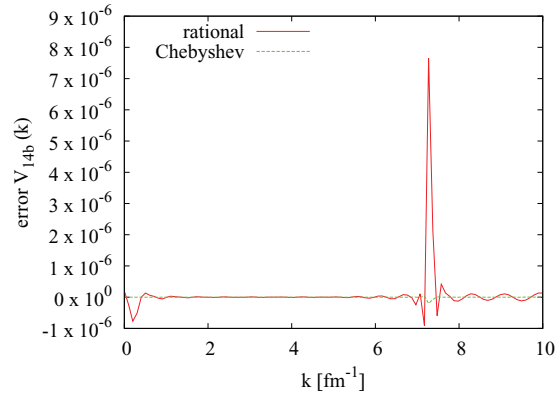

FIG. 16. (Color online) $\Delta V_{14b\,\mathrm{rational}}(k)$, $\Delta V_{14b\,\mathrm{Chebyshev}}(k)$.

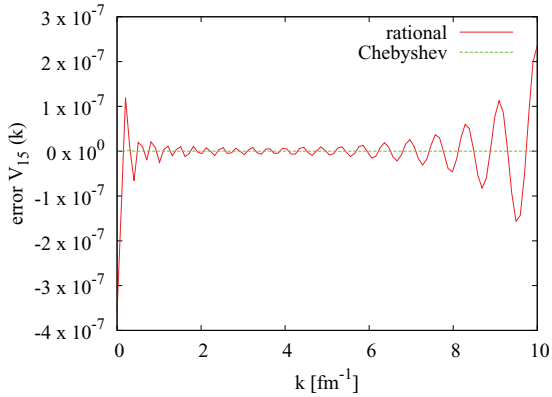

FIG. 17. (Color online) $\Delta V_{15\,\mathrm{rational}}(k)$, $\Delta V_{15\,\mathrm{Chebyshev}}(k)$.

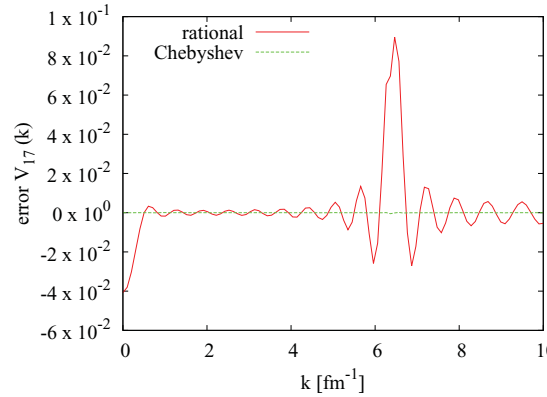

FIG. 19. (Color online) $\Delta V_{17\,\mathrm{rational}}(k)$, $\Delta V_{17\,\mathrm{Chebyshev}}(k)$.

These results are shown in Tables IV, V, VI, and VII for all 24 operators and a representative range of the momentum transfers. The columns labeled RFExp show the scalar potential functions using the rational function expansion, the columns labeled CExp show the same quantities using the Chebyshev expansion, while the columns labeled NFT show the results of the direct numerical Fourier transform. Figures 3–26 plot the difference of the approximate Fourier transforms with an accurate Fourier Bessel transform divided by half of the sum of these quantities. The solid curves are for the rational function expansion and the dotted curved are for the Chebyshev expansion.

These tables show generally good agreement among the three methods of computation. At 1 fm^{-1} and 5 fm^{-1} the Chebyshev expansion agrees with the direct numerical Fourier transform to between 5-7 significant figures for all 24 potentials. There is similar agreement at 15 fm^{-1} and 25 fm^{-1} except in potentials 17. The agreement between the potentials calculated using the rational function expansion do not agree with the direct numerical Fourier transforms as well as the Chebyshev expansion. The accuracy depends on the particular potential and gets worse as the momentum transfer increases. Thus for precision calculations the Chebyshev expansion is preferred.

Figures 3–26 provide a more complete picture of the nature of the errors in both approximations. Spikes in the errors occur near points where the potentials change sign. Some of the errors near zero are enhanced because the some of the plotted potentials are divided by powers of the momentum transfer. For these terms the operators include compensating powers of the momentum transfer that vanish near the origin, so the contribution of the error in the full potential near the origin is reduced. The rational function expansions have larger relative errors near higher and lower values of the momentum transfer. This is not surprising because the basis functions are not local. The Chebyshev expansion is uniformly good, in part because it is a local expansion, so more intervals can be added as needed. The largest errors are in potential 17. At 10 fm^{-1} its value is about -1.2×10^{-8}, which is several orders of magnitude smaller than any of the other potentials at that momentum transfer.

As a second test the deuteron binding energy and wave functions computed using the two different momentum-space potentials are compared to each other and to the direct Fourier transform of wave functions computed using a configuration-space partial-wave calculation. The deuteron binding energy and the s and d wave functions are computed using the operator form of the Fourier transformed potential, by direct integration of the vector variables. The method of solution, which is discussed in Ref. [10], uses the expansion in Eq. (1.7) directly without using partial waves. Calculations are performed for both the Chebyshev and rational-function representations of the momentum space potentials.

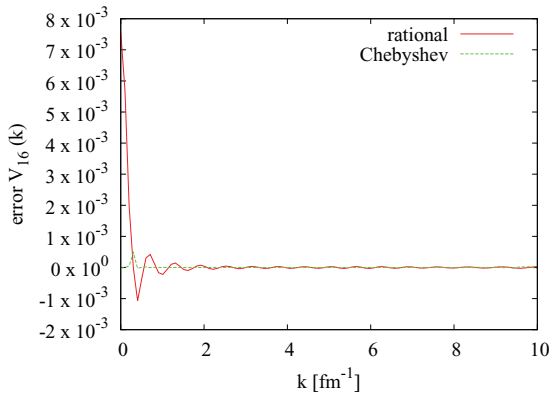

FIG. 18. (Color online) $\Delta V_{16\,\mathrm{rational}}(k)$, $\Delta V_{16\,\mathrm{Chebyshev}}(k)$.

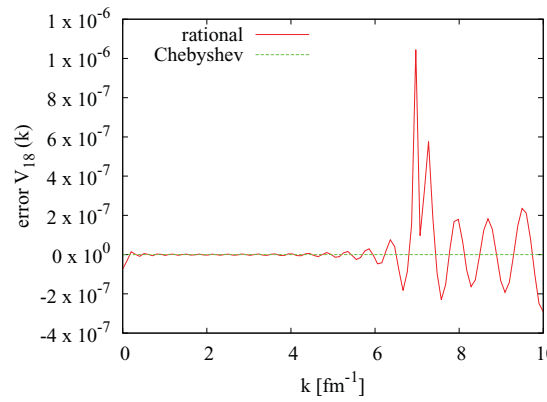

FIG. 20. (Color online) $\Delta V_{18\,\mathrm{rational}}(k)$, $\Delta V_{18\,\mathrm{Chebyshev}}(k)$.

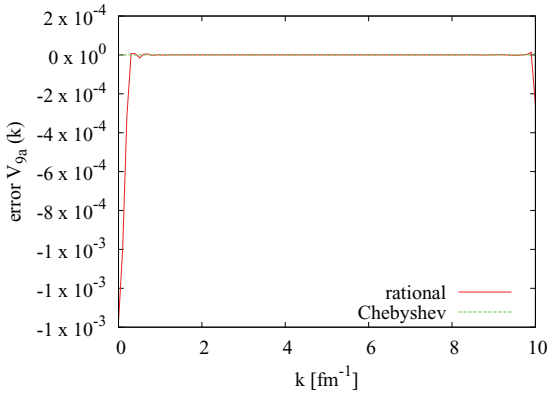

FIG. 21. (Color online) $\Delta V_{9a\,\mathrm{rational}}(k)$, $\Delta V_{9a\,\mathrm{Chebyshev}}(k)$.

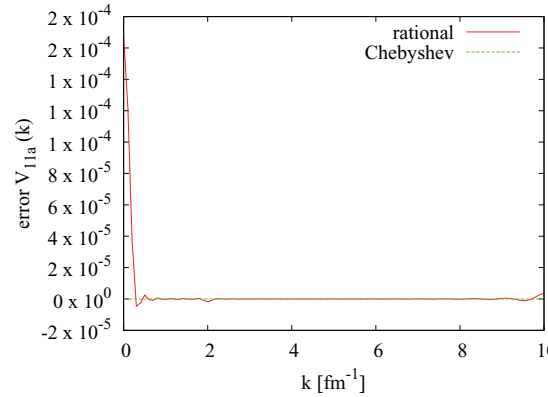

FIG. 23. (Color online) $\Delta V_{11a\,\mathrm{rational}}(k)$, $\Delta V_{11a\,\mathrm{Chebyshev}}(k)$.

These calculations are compared to a configuration-space partial-wave calculation. In that calculation, labeled pw in Table VIII, the wave functions are represented by an expansion in 70 configuration-space basis functions using the configuration-space basis functions in Eq. (3.5). Matrix elements of the partial-wave projection of the Hamiltonian, with the configuration-space Argonne V18 potential, are computed in this basis and the eigenvalue problem is solved numerically. The Fourier transform is computed by analytically Fourier transforming the basis functions. The solution of the eigenvalue problem gives an independent evaluation of both the binding energy and wave functions constructed directly from the configuration space potential.

The deuteron binding energy obtained using the Chebyshev representation of the Fourier transform gives a deuteron binding energy of $E_d = -2.242233$ MeV. The rational function representation gives a deuteron binding energy of $E_d = -2.242193$ MeV compared with $E_d = -2.242211$ MeV using the configuration-space partial-wave calculation. The binding energies based on all three calculations agree to within 22 eV. The computation used in the configuration-space partial-wave calculation is a Galerkin calculation and thus gives a variational bound on the binding energy.

These eigenvalues differ from the experimental deuteron binding energy. This is because the momentum-space potentials used in these computations do not include electromagnetic corrections that appear in the Argonne V18 codes. The electromagnetic corrections contribute an additional 17.6 keV [11] to the binding energy, which is consistent with the experimental binding energy of -2.2246 MeV.

The s and d wave functions for all three calculations are compared in Table VIII. The wave functions differ in the fifth or sixth significant figure, while binding energies of all three calculations differ in the sixth significant figure.

The electromagnetic contributions to the Argonne V18 potential are important for low-energy high-precision calculations. The Fourier transform of the electromagnetic contributions of the Argonne V18 potential can be computed analytically, and can be added to the strong interaction contribution discussed in this paper when necessary. The analytic Fourier transform of the electromagnetic contribution is discussed in Appendix C.

While this paper gives the momentum-space version of the operator expansion of the Argonne V18 potential, it is often useful to have partial-wave contributions of the potential. These can be computed from the operator matrix elements using a one-dimensional integration over the cosine of the angle between the initial and final momenta. A simple method to compute the partial-wave projections from the operator expansion is given in Appendix B. The programs to compute the potentials $\tilde{V}_m(q)$ using both methods are available as supplementary material to the electronic version of this article.

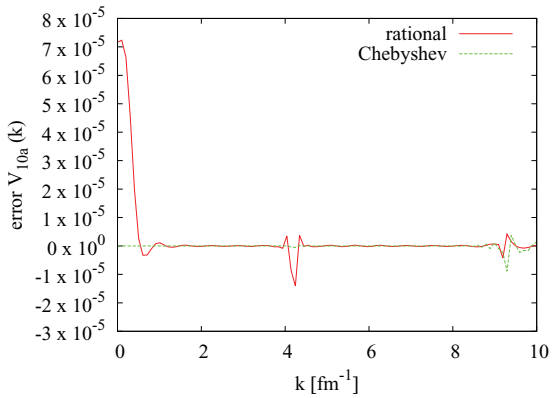

FIG. 22. (Color online) $\Delta V_{10a\,\mathrm{rational}}(k)$, $\Delta V_{10a\,\mathrm{Chebyshev}}(k)$.

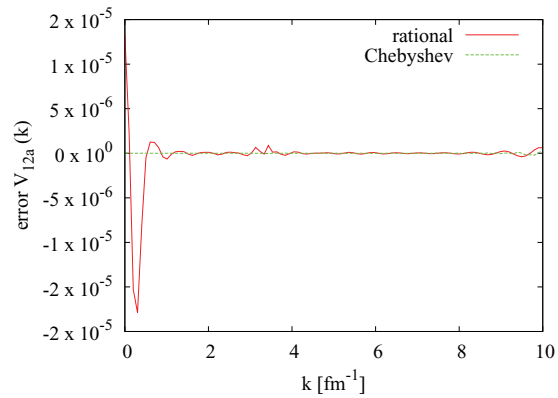

FIG. 24. (Color online) $\Delta V_{12a\,\mathrm{rational}}(k)$, $\Delta V_{12a\,\mathrm{Chebyshev}}(k)$.

TABLE VIII. Deuteron s and d wave functions using Chebyshev expansion, rational function expansion, and r-space partial waves.

k fm^{-1}	$u_s(k)$ (CExp)	$u_s(k)$ (RFExp)	$u_s(k)$ (pw)	$u_d(k)$ (CExp)	$u_d(k)$ (RFExp)	$u_d(k)$ (pw)
0.0	1.2695×10^{1}	1.2695×10^{1}	1.2693×10^{1}	0.00000×10^{0}	0.00000×10^{0}	0.00000×10^{0}
0.5	1.9609×10^{0}	1.9609×10^{0}	1.9609×10^{0}	-2.19827×10^{-1}	-2.19811×10^{-1}	-2.19826×10^{-1}
1.0	3.7684×10^{-1}	3.7685×10^{-1}	3.7684×10^{-1}	-1.72164×10^{-1}	-1.72159×10^{-1}	-1.72164×10^{-1}
1.5	8.2472×10^{-2}	8.2472×10^{-2}	8.2471×10^{-2}	-1.12429×10^{-1}	-1.12429×10^{-1}	-1.12429×10^{-1}
2.0	6.0809×10^{-3}	6.0808×10^{-3}	6.0806×10^{-3}	-7.10857×10^{-2}	-7.10863×10^{-2}	-7.10857×10^{-2}
2.5	-1.3615×10^{-2}	-1.3616×10^{-2}	-1.3615×10^{-2}	-4.45428×10^{-2}	-4.45432×10^{-2}	-4.45428×10^{-2}
3.0	-1.6153×10^{-2}	-1.6153×10^{-2}	-1.6153×10^{-2}	-2.76853×10^{-2}	-2.76854×10^{-1}	-2.76853×10^{-2}
3.5	-1.3648×10^{-2}	-1.3648×10^{-2}	-1.3648×10^{-2}	-1.69880×10^{-2}	-1.69881×10^{-2}	-1.69881×10^{-2}
4.0	-1.0153×10^{-2}	-1.0153×10^{-2}	-1.0153×10^{-2}	-1.02233×10^{-2}	-1.02234×10^{-2}	-1.02234×10^{-2}
4.5	-6.9954×10^{-3}	-6.9954×10^{-3}	-6.9953×10^{-3}	-5.98472×10^{-3}	-5.98475×10^{-3}	-5.98472×10^{-3}
5.0	-4.5270×10^{-3}	-4.5270×10^{-3}	-4.5270×10^{-3}	-3.37040×10^{-3}	-3.37043×10^{-3}	-3.37041×10^{-3}

ACKNOWLEDGMENTS

This work supported by the US Department of Energy, Contract No. DE-FG02-86ER40286 and National Science Foundation Grants No. NSF-PHY-1005578 and No. NSF-PHY-1005501. The authors would like to acknowledge useful comments from Professor C. Elster in preparing this manuscript.

APPENDIX A

In this appendix we compute the Fourier transform of the parts of the potential containing the five types of operators, $\mathbf{I}$, $\mathbf{L}\cdot\mathbf{S}$, $\mathbf{L}\cdot\mathbf{L}$,$(\mathbf{L}\cdot\mathbf{S})^2$, and S_{12} that appear in Eqs. (1.3)–(1.6).

$\mathbf{L}\cdot\mathbf{S}$:

Let $\mathbf{q} := \mathbf{k}' - \mathbf{k}$.

The Fourier transform is

$$\begin{aligned}
&\frac{1}{(2\pi)^3}\int e^{-i\mathbf{k}'\cdot\mathbf{r}} V_j(r)\mathbf{L}\cdot\mathbf{S} e^{i\mathbf{k}\cdot\mathbf{r}} d\mathbf{r} \\
&\quad = \frac{1}{(2\pi)^3}\int e^{-i\mathbf{k}'\cdot\mathbf{r}} V_j(r)\mathbf{S}\cdot(\mathbf{r}\times\mathbf{p}) e^{i\mathbf{k}\cdot\mathbf{r}} d\mathbf{r} \\
&\quad = \frac{1}{(2\pi)^3}\int e^{-i\mathbf{k}'\cdot\mathbf{r}} V_j(r)\mathbf{S}\cdot(\mathbf{r}\times\mathbf{k}) e^{i\mathbf{k}\cdot\mathbf{r}} d\mathbf{r} \\
&\quad = \frac{1}{(2\pi)^3}\int e^{-i\mathbf{q}\cdot\mathbf{r}} V_j(r)\mathbf{S}\cdot(\mathbf{r}\times\mathbf{k}) d\mathbf{r} \\
&\quad = \frac{4\pi}{(2\pi)^3}\int \sum_{l=0}^{\infty}\sum_{m=-l}^{l} (-i)^l j_l(qr) Y_{lm}(\hat{\mathbf{q}}) Y_{lm}^*(\hat{\mathbf{r}}) \\
&\qquad \times V_j(r)\mathbf{S}\cdot(\mathbf{r}\times\mathbf{k}) d\mathbf{r}. \qquad \text{(A1)}
\end{aligned}$$

Since $\mathbf{r}$ can be expanded as a linear combination of spherical harmonics, $Y_{1m}(\hat{\mathbf{r}})$, the only terms that survive are the $l = 1$ terms. The integral over angles and the spherical harmonics replace $\hat{\mathbf{r}}$ by $\hat{\mathbf{q}}$, giving

$$\begin{aligned}
&-\frac{4\pi i}{(2\pi)^3}\int_0^{\infty} j_1(qr) V_j(r)\mathbf{S}\cdot(\mathbf{q}\times\mathbf{k}) r^3 dr \\
&\quad = i\mathbf{S}\cdot(\mathbf{k}\times\mathbf{k}')\times\left[\frac{1}{2\pi^2 q}\int_0^{\infty} j_1(qr) V_j(r) r^3 dr\right]. \qquad \text{(A2)}
\end{aligned}$$

Thus the Fourier transform has the form

$$\frac{1}{(2\pi)^3}\int e^{-i\mathbf{k}'\cdot\mathbf{r}} V_j(r)\mathbf{L}\cdot\mathbf{S} e^{i\mathbf{k}\cdot\mathbf{r}} d\mathbf{r} = i\mathbf{S}\cdot(\mathbf{k}\times\mathbf{k}') I_1(q) \qquad \text{(A3)}$$

where

$$I_1(q) := \frac{1}{2\pi^2 q}\int_0^{\infty} j_1(qr) V_j(r) r^3 dr. \qquad \text{(A4)}$$

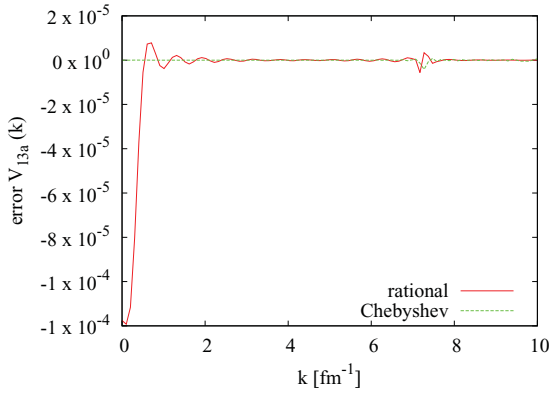

FIG. 25. (Color online) $\Delta V_{13a\,\text{rational}}(k)$, $\Delta V_{13a\,\text{Chebyshev}}(k)$.

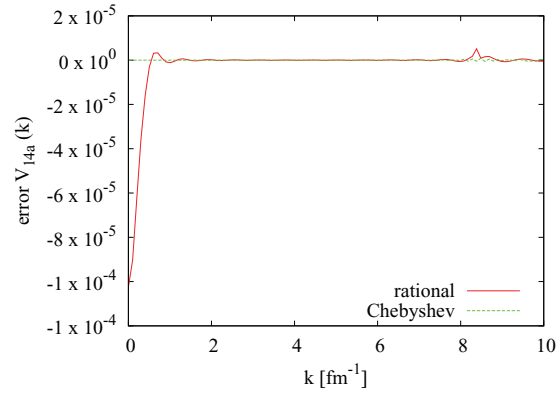

FIG. 26. (Color online) $\Delta V_{14a\,\text{rational}}(k)$, $\Delta V_{14a\,\text{Chebyshev}}(k)$.

The following relations are used to compute Fourier transforms of the remaining three operators:

$$\nabla_q f(q) = f'(q)\frac{\mathbf{q}}{q} \tag{A5}$$

$$\nabla_q^2 f(q) = f''(q) + \frac{2}{q}f'(q) \tag{A6}$$

$$(\mathbf{a}\cdot\nabla_q)(\mathbf{b}\cdot\nabla_q)f(q) = \frac{\mathbf{a}\cdot\mathbf{q}}{q}\frac{\mathbf{b}\cdot\mathbf{q}}{q}\left[f''(q) - \frac{f'(q)}{q}\right] + \frac{\mathbf{a}\cdot\mathbf{b}}{q}f'(q). \tag{A7}$$

$\mathbf{L}\cdot\mathbf{L}$:
The Fourier transform of this operator is

$$\begin{aligned}
&\frac{1}{(2\pi)^3}\int e^{-i\mathbf{k}'\cdot\mathbf{r}}V_j(r)(\mathbf{r}\times\mathbf{p})\cdot(\mathbf{r}\times\mathbf{p})e^{i\mathbf{k}\cdot\mathbf{r}}d\mathbf{r}\\
&= \frac{1}{(2\pi)^3}\int e^{-i\mathbf{k}'\cdot\mathbf{r}}V_j(r)(\mathbf{r}\times\mathbf{k}')\cdot(\mathbf{r}\times\mathbf{k})e^{i\mathbf{k}\cdot\mathbf{r}}d\mathbf{r}\\
&= (i\nabla_q\times\mathbf{k}')\cdot(i\nabla_q\times\mathbf{k})\frac{1}{(2\pi)^3}\int V_j(r)e^{-i\mathbf{q}\cdot\mathbf{r}}d\mathbf{r}\\
&= -(\nabla_q\times\mathbf{k}')\cdot(\nabla_q\times\mathbf{k})\frac{4\pi}{(2\pi)^3}\int_0^\infty V_j(r)j_0(qr)r^2dr.
\end{aligned} \tag{A8}$$

To compute the derivatives use

$$(\nabla_q\times\mathbf{k}')\cdot(\nabla_q\times\mathbf{k}) = (\mathbf{k}\cdot\mathbf{k}')(\nabla_q\cdot\nabla_q) - (\mathbf{k}\cdot\nabla_q)(\mathbf{k}\cdot\nabla_q)$$

in the above to get

$$\begin{aligned}
&-(\nabla_q\times\mathbf{k}')\cdot(\nabla_q\times\mathbf{k})\frac{4\pi}{(2\pi)^3}\int_0^\infty V_j(r)j_0(qr)r^2dr\\
&= -\left[(\mathbf{k}'\cdot\mathbf{k})\nabla_q^2 - (\mathbf{k}'\cdot\nabla_q)(\mathbf{k}\cdot\nabla_q)\right]I_0(q)
\end{aligned} \tag{A9}$$

where

$$\begin{aligned}
I_0(q) &= \frac{4\pi}{(2\pi)^3}\int_0^\infty V_j(r)j_0(qr)r^2dr\\
&= \frac{1}{2\pi^2}\int_0^\infty V_j(r)j_0(qr)r^2dr.
\end{aligned} \tag{A10}$$

Evaluating this gives

$$\begin{aligned}
&-\left[(\mathbf{k}'\cdot\mathbf{k})\nabla_q^2 - (\mathbf{k}'\cdot\nabla_q)(\mathbf{k}\cdot\nabla_q)\right]I_0(q)\\
&= -(\mathbf{k}'\cdot\mathbf{k})\left[I_0''(q) + \frac{1}{q}I_0'(q)\right] + \frac{(\mathbf{k}'\cdot\mathbf{q})(\mathbf{k}\cdot\mathbf{q})}{q^2}\\
&\quad\times\left[I_0''(q) - \frac{1}{q}I_0'(q)\right].
\end{aligned} \tag{A11}$$

To eliminate the derivatives use

$$\begin{aligned}
&I_0''(q) - \frac{1}{q}I_0'(q)\\
&= \frac{1}{2\pi^2}\int_0^\infty V(r)\left[j_0''(qr) - j_0'(qr)\frac{1}{qr}\right]r^4dr\\
&= \frac{1}{2\pi^2}\int_0^\infty V(r)j_2(qr)r^4dr = I_2(q)
\end{aligned}$$

and

$$\begin{aligned}
&I_0''(q) + \frac{1}{q}I_0'(q)\\
&= \frac{1}{2\pi^2}\int_0^\infty V(r)\left[j_0''(qr) - j_0'(qr)\frac{1}{qr} + 2j_0'(qr)\frac{1}{qr}\right]r^4dr\\
&= \frac{1}{2\pi^2}\int_0^\infty V(r)j_2''(qr)r^4dr - \frac{1}{2\pi^2}\frac{2}{q}\int_0^\infty V(r)j_1(qr)r^3dr\\
&= I_2(q) - \frac{2}{q}I_1(q).
\end{aligned}$$

This gives

$$\begin{aligned}
&\frac{1}{(2\pi)^3}\int e^{-i\mathbf{k}'\cdot\mathbf{r}}V_j(r)(\mathbf{r}\times\mathbf{p})\cdot(\mathbf{r}\times\mathbf{p})e^{i\mathbf{k}\cdot\mathbf{r}}d\mathbf{r}\\
&= -(\mathbf{k}'\cdot\mathbf{k})\left[I_2(q) - \frac{2}{q}I_1(q)\right] + \frac{(\mathbf{k}'\cdot\mathbf{q})(\mathbf{k}\cdot\mathbf{q})}{q^2}I_2(q)
\end{aligned} \tag{A12}$$

which can be reexpressed in terms of cross products

$$\begin{aligned}
&\frac{1}{(2\pi)^3}\int e^{-i\mathbf{k}'\cdot\mathbf{r}}V_j(r)(\mathbf{r}\times\mathbf{p})\cdot(\mathbf{r}\times\mathbf{p})e^{i\mathbf{k}\cdot\mathbf{r}}d\mathbf{r}\\
&= -I_2(q)\frac{(\mathbf{k}'\times\mathbf{k})\cdot(\mathbf{k}'\times\mathbf{k})}{q^2} + \frac{2}{q}(\mathbf{k}'\cdot\mathbf{k})I_1(q).
\end{aligned} \tag{A13}$$

$(\mathbf{L}\cdot\mathbf{S})^2$:
The Fourier transform is

$$\begin{aligned}
&\frac{1}{(2\pi)^3}\int e^{-i(\mathbf{k}'-\mathbf{k})\cdot\mathbf{r}}V_j(r)(\mathbf{L}\cdot\mathbf{S})^2d\mathbf{r}\\
&= \frac{1}{(2\pi)^3}\int e^{-i(\mathbf{k}'-\mathbf{k})\cdot\mathbf{r}}V_j(r)\left[\mathbf{S}\cdot(\mathbf{r}\times\mathbf{p})\right]^2d\mathbf{r}\\
&= -\frac{4\pi}{(2\pi)^3}[(\mathbf{k}'\times\mathbf{S})\cdot\nabla_q][(\mathbf{k}\times\mathbf{S})\cdot\nabla_q]\int j_0(qr)V_j(r)r^2dr\\
&= -[(\mathbf{k}'\times\mathbf{S})\cdot\nabla_q)][(\mathbf{k}\times\mathbf{S})\cdot\nabla_q]I_0(q)\\
&= -\{(\mathbf{k}'\times\mathbf{S})\cdot\mathbf{q}[(\mathbf{k}\times\mathbf{S})\cdot\mathbf{q}]\}\frac{1}{q^2}\left[I_0''(q) - \frac{1}{q}I_0'(q)\right]\\
&\quad -(\mathbf{k}'\times\mathbf{S})\cdot(\mathbf{k}\times\mathbf{S})\frac{1}{q}I_0'(q)
\end{aligned}$$

$$= -\{(\mathbf{k}' \times \mathbf{S}) \cdot \mathbf{q}[(\mathbf{k} \times \mathbf{S}) \cdot \mathbf{q}]\} = \frac{1}{q^2} I_2(q) + (\mathbf{k}' \times \mathbf{S}) \cdot (\mathbf{k} \times \mathbf{S}) \frac{1}{q} I_1(q) \tag{A14}$$

which gives

$$-[\mathbf{S} \cdot (\mathbf{k} \times \mathbf{k}')]^2 \frac{1}{q^2} I_2(q) + (\mathbf{k}' \times \mathbf{S}) \cdot (\mathbf{k} \times \mathbf{S}) \frac{1}{q} I_1(q) \tag{A15}$$

or

$$\frac{1}{(2\pi)^2} \int e^{-i(\mathbf{k}'-\mathbf{k})} V_j(r) (\mathbf{L} \cdot \mathbf{S})^2 d\mathbf{r} = -[\mathbf{S} \cdot (\mathbf{k} \times \mathbf{k}')]^2 \frac{1}{q^2} I_2(q) + (\mathbf{k}' \times \mathbf{S}) \cdot (\mathbf{k} \times \mathbf{S}) \frac{1}{q} I_1(q). \tag{A16}$$

$\frac{1}{3} S_{12} = \left[(\hat{\mathbf{r}} \cdot \boldsymbol{\sigma}_1)(\hat{\mathbf{r}} \cdot \boldsymbol{\sigma}_2) - \frac{1}{3} \boldsymbol{\sigma}_1 \cdot \boldsymbol{\sigma}_2\right]$:
The Fourier transform is

$$\begin{aligned}
&\frac{1}{(2\pi)^3} \int e^{-i\mathbf{k}' \cdot \mathbf{r}} V(r) \left((\hat{\mathbf{r}} \cdot \boldsymbol{\sigma}_1)(\hat{\mathbf{r}} \cdot \boldsymbol{\sigma}_2) - \frac{1}{3} \boldsymbol{\sigma}_1 \cdot \boldsymbol{\sigma}_2 \right) e^{i\mathbf{k} \cdot \mathbf{r}} d\mathbf{r} \\
&= -\left((\nabla_q \cdot \boldsymbol{\sigma}_1)(\nabla_q \cdot \boldsymbol{\sigma}_2) - \frac{1}{3} \boldsymbol{\sigma}_1 \cdot \boldsymbol{\sigma}_2 \nabla_q^2 \right) \frac{4\pi}{(2\pi)^3} \\
&\quad \times \int V(r) \frac{r^2}{r^2} j_0(qr) dr \\
&= -\frac{\boldsymbol{\sigma}_1 \cdot \mathbf{q}}{q} \frac{\boldsymbol{\sigma}_2 \cdot \mathbf{q}}{q} \left[I''_{0-}(q) - \frac{I'_{0-}(q)}{q} \right] - \frac{\mathbf{s}_1 \cdot \mathbf{s}_2}{q} I'_0(q) \\
&= +\frac{1}{3} \boldsymbol{\sigma}_1 \cdot \boldsymbol{\sigma}_2 \left[I''_{0-}(q) + \frac{2}{q} I'_{0-}(q) \right].
\end{aligned} \tag{A17}$$

Thus,

$$\begin{aligned}
&\frac{1}{(2\pi)^3} \int e^{-i\mathbf{k}' \cdot \mathbf{r}} V(r) \left[3(\hat{\mathbf{r}} \cdot \boldsymbol{\sigma}_1)(\hat{\mathbf{r}} \cdot \boldsymbol{\sigma}_2) - \boldsymbol{\sigma}_1 \cdot \boldsymbol{\sigma}_2 \right] e^{i\mathbf{k} \cdot \mathbf{r}} d\mathbf{r} \\
&= -\left(3 \frac{\boldsymbol{\sigma}_1 \cdot \mathbf{q}}{q} \frac{\boldsymbol{\sigma}_2 \cdot \mathbf{q}}{q} - \boldsymbol{\sigma}_1 \cdot \boldsymbol{\sigma}_2 \right) I_{2-}(q)
\end{aligned} \tag{A18}$$

where

$$I_{0-}(q) = \frac{4\pi}{(2\pi)^3} \int V(r) j_2(qr) r^2 dr. \tag{A19}$$

APPENDIX B

In this appendix we compute the partial-wave projection of potentials from the vector representation of the momentum-space potential. Using rotational invariance the partial-wave potentials can be expressed using a one-dimensional integral over the cosine of the angle between the initial and final momentum vectors. The method below is similar to the method first proposed in Ref. [12].

Rotational invariance of the potential implies

$$\begin{aligned}
&\langle j, \mu, k, l, s | V | j', \mu', k', l', s' \rangle \\
&= \langle j, \mu, k, l, s | U^\dagger(R) V U(R) | j', \mu', k', l', s' \rangle \\
&= \sum_{\nu\nu'} D^{j*}_{\nu\mu}(R) D^{j}_{\nu'\mu'}(R) \langle j, \nu, k, l, s | V | j', \nu', k', l', s' \rangle \\
&= \int dR \sum_{\nu\nu'} D^{j*}_{\nu\mu}(R) D^{j}_{\nu'\mu'}(R) \langle j, \nu, k, l, s | V | j', \nu', k', l', s' \rangle \\
&= \delta_{jj'} \sum_{\mu'\nu'} \delta_{\mu\mu'} \frac{\delta_{\nu\nu'}}{2j+1} \langle j, \nu, k, l, s | V | j', \nu', k', l', s' \rangle \\
&= \delta_{\mu\mu'} \delta_{jj'} \langle k, l, s \| V^j \| k', l', s' \rangle
\end{aligned} \tag{B1}$$

where we have integrated over the $SU(2)$ Haar measure with normalization $\int dR = 1$ and defined the partial-wave potentials by

$$\langle k, l, s \| V^j \| k', l', s' \rangle := \frac{1}{2j+1} \sum_{\mu=-j}^{j} \sum_{m_l m'_l} \sum_{m_s m'_s} \langle j, \mu, k, l, s | V | j, \mu, k', l', s' \rangle. \tag{B2}$$

This kernel is rotationally invariant. Formally the partial-wave potential is

$$\begin{aligned}
&\langle k, l, s \| V^j \| k', l', s' \rangle \\
&= \int d\hat{\mathbf{k}} d\hat{\mathbf{k}}' \frac{1}{2j+1} \sum_{\mu=-j}^{j} \left\langle \frac{1}{2}, \mu_1, \frac{1}{2}, \mu_2 \middle| s, m_s \right\rangle \\
&\times \langle l, m_l, s, m_s | j, \mu \rangle Y^*_{lm_l}(\hat{\mathbf{k}}) \langle \mathbf{k}, \mu_1, \mu_2 \| V \| \mathbf{k}', \mu'_1, \mu'_2 \rangle \\
&\times \left\langle \frac{1}{2}, \mu'_1, \frac{1}{2}, \mu'_2 \middle| s', m'_s \right\rangle \langle l', m'_l, s', m'_s | j, \mu \rangle Y_{l'm'_l}(\hat{\mathbf{k}}').
\end{aligned} \tag{B3}$$

For any fixed rotation, R, rotational invariance of V gives

$$\begin{aligned}
&\langle \mathbf{k}, \mu_1, \mu_2 \| V \| \mathbf{k}', \mu'_1, \mu'_2 \rangle \\
&= \langle \mathbf{k}, \mu_1, \mu_2 \| U^\dagger(R) V U(R) \| \mathbf{k}', \mu'_1, \mu'_2 \rangle \\
&= \sum_{\mu''_1\mu''_2} \sum_{\mu'''_1\mu'''_2} D^{*1/2}_{\mu''_1\mu_1}(R) D^{*1/2}_{\mu''_2\mu_2}(R) \langle R\mathbf{k}, \mu''_1, \mu''_2 \| V \| \\
&\quad \times R\mathbf{k}', \mu'''_1, \mu'''_2 \rangle D^{1/2}_{\mu'''_1\mu'_1}(R) D^{1/2}_{\mu'''_2\mu'_2}(R).
\end{aligned} \tag{B4}$$

Using this expression in Eq. (B3) gives

$$\begin{aligned}
&\langle k, l, s \| V^j \| k', l', s' \rangle \\
&= \int d\hat{\mathbf{k}} d\hat{\mathbf{k}}' \frac{1}{2j+1} \sum_{\mu=-j}^{j} \left\langle \frac{1}{2}, \mu_1, \frac{1}{2}, \mu_2 \middle| s, m_s \right\rangle \\
&\times \langle l, m_l, s, m_s | j\mu \rangle \langle Y^*_{lm_l}(\hat{\mathbf{k}}) D^{*1/2}_{\mu''_1\mu_1}(R) D^{*1/2}_{\mu''_2\mu_2}(R) \\
&\times \langle R\mathbf{k}, \mu''_1, \mu''_2 \| V \| R\mathbf{k}', \mu'''_1, \mu'''_2 \rangle D^{1/2}_{\mu'''_1\mu'_1}(R) D^{1/2}_{\mu'''_2\mu'_2} \\
&\times (R) \left\langle \frac{1}{2}, \mu'_1, \frac{1}{2}, \mu'_2 \middle| s', m'_s \right\rangle \langle l', m'_l, s', m'_s | j\mu \rangle \langle Y_{l'm'_l}(\hat{\mathbf{k}}').
\end{aligned} \tag{B5}$$

Next we eliminate three of the integrals in the potential matrix. For any fixed $\mathbf{k}'$ there is an R such that $R(k')\hat{\mathbf{k}}' = \hat{\mathbf{z}}$. Obviously $R^{-1}(k') = R_z(\phi') R_y(\theta') R_z(\xi)$ where (θ', ϕ') are the

polar angles of $\mathbf{k}'$ and ξ is arbitrary has this property where

$$R_y(\theta) = \begin{pmatrix} \cos(\theta) & 0 & \sin(\theta) \\ 0 & 1 & \\ -\sin(\theta) & 0 & \cos(\theta) \end{pmatrix} \tag{B6}$$

$$R_z(\phi) = \begin{pmatrix} \cos(\phi) & -\sin(\phi) & 0 \\ \sin(\phi) & \cos(\phi) & 0 \\ 0 & 0 & 1 \end{pmatrix}. \tag{B7}$$

In this case

$$R\mathbf{k}' = k'\hat{\mathbf{z}} \tag{B8}$$

and

$$R\mathbf{k} = R_z^{-1}(\xi)R_y^{-1}(\theta')R_z^{-1}(\phi')\mathbf{k}. \tag{B9}$$

For fixed $\mathbf{k}'$ define $\mathbf{k}''$ by

$$\mathbf{k}'' = R_y^{-1}(\theta')R_z^{-1}(\phi')\mathbf{k}. \tag{B10}$$

Given these fixed (primed) angles we change the unprimed integration variables $\mathbf{k} \to \mathbf{k}''$. We also have

$$R\mathbf{k} = R_z^{-1}(\xi)\mathbf{k}'' \tag{B11}$$

We are also free to choose the angle ξ in $R_z^{-1}(\xi)$. We choose it so it transforms $\mathbf{k}''$ to the $x-z$ plane. This is achieved by letting ξ be the azimuthal angle of $\mathbf{k}'''$

$$R_z^{-1}(\phi'') = \begin{pmatrix} \cos(\phi'') & \sin(\phi'') & 0 \\ -\sin(\phi'') & \cos(\phi'') & 0 \\ 0 & 0 & 1 \end{pmatrix} \tag{B12}$$

$$R_z^{-1}(\phi'')\mathbf{k}'' = \begin{pmatrix} \cos(\phi'') & \sin(\phi'') & 0 \\ -\sin(\phi'') & \cos(\phi'') & 0 \\ 0 & 0 & 1 \end{pmatrix} \begin{pmatrix} k''\sin(\theta'')\cos(\phi'') \\ k''\sin(\theta'')\sin(\phi'') \\ k''\cos(\theta'') \end{pmatrix} = \begin{pmatrix} k''\sin(\theta'') \\ 0 \\ k''\cos(\theta'') \end{pmatrix}. \tag{B13}$$

With these substitutions the partial wave integral becomes

$$\begin{aligned}
\langle k,l,s\|V^j\|k',l',s'\rangle &= \int d\hat{\mathbf{k}}''d\hat{\mathbf{k}}'\frac{1}{2j+1}\sum_{\mu=-j}^{j}\left\langle \frac{1}{2},\mu_1,\frac{1}{2},\mu_2\middle|s,m_s\right\rangle\langle l,m_l,s,m_s|j,\mu\rangle Y^*_{lm}[R^{-1}R_z^{-1}(\phi'')\hat{\mathbf{k}}''] \\
&\quad\times D^{*1/2}_{\mu_1''\mu_1}(R)D^{*1/2}_{\mu_2''\mu_2}(R)\langle k''[\hat{\mathbf{x}}\sin(\theta'')+\hat{\mathbf{z}}\cos(\theta'')],\mu_1'',\mu_2''\|V\|k'\hat{\mathbf{z}},\mu_1''',\mu_2'''\rangle D^{1/2}_{\mu_1'''\mu_1'}(R)D^{1/2}_{\mu_2'''\mu_2'}(R) \\
&\quad\times\left\langle \frac{1}{2},\mu_1',\frac{1}{2},\mu_2'\middle|s',m_s'\right\rangle\langle l',m_l',s',m_s'|j,\mu\rangle\langle Y_{l'm_l'}(R^{-1}\hat{\mathbf{z}}') \\
&= \int d\hat{\mathbf{k}}''d\hat{\mathbf{k}}'\frac{1}{2j+1}\sum_{\mu=-j}^{j}\left\langle \frac{1}{2},\mu_1,\frac{1}{2},\mu_2\middle|s,m_s\right\rangle\langle l,m_l,s,m_s|j,\mu\rangle Y^*_{lm}[\hat{\mathbf{x}}\sin(\theta'')+\hat{\mathbf{z}}\cos(\theta'')]D^{l*}_{m_l''m_l}(R) \\
&\quad\times D^{*1/2}_{\mu_1''\mu_1}(R)D^{*1/2}_{\mu_2''\mu_2}(R)\langle k''[\hat{\mathbf{x}}\sin(\theta'')+\hat{\mathbf{z}}\cos(\theta'')],\mu_1'',\mu_2''\|V\|k'\hat{\mathbf{z}},\mu_1''',\mu_2'''\rangle D^{1/2}_{\mu_1'''\mu_1'}(R)D^{1/2}_{\mu_2'''\mu_2'}(R) \\
&\quad\times\left\langle \frac{1}{2},\mu_1',\frac{1}{2},\mu_2'\middle|s',m_s'\right\rangle\langle l',m_l',s',m_s'|j\mu\rangle Y_{l'm_l'}(\hat{\mathbf{z}})D^{l'}_{m_l'''m_l'}(R).
\end{aligned} \tag{B14}$$

Using properties of Clebsch-Gordan coefficients [i.e., $D(R) < | > = < | > D(R) \otimes D(R)$] we get

$$\begin{aligned}
&\langle k,l,s\|V^j\|k',l',s'\rangle \\
&= \int d\hat{\mathbf{k}}''d\hat{\mathbf{k}}'\frac{1}{2j+1}\sum_{\mu=-j}^{j}D^{j*}_{\mu''\mu}(R)\left\langle \frac{1}{2},\mu_1,\frac{1}{2},\mu_2\middle|s,m_s\right\rangle\langle l,m_l,s,m_s|j,\mu\rangle Y^*_{lm_l}[\hat{\mathbf{x}}\sin(\theta'')+\hat{\mathbf{z}}\cos(\theta'')|l,m_l] \\
&\quad\times\langle k''[\hat{\mathbf{x}}\sin(\theta'')+\hat{\mathbf{z}}\cos(\theta'')],\mu_1,\mu_2\|V\|k'\hat{\mathbf{z}},\mu_1',\mu_2'\rangle\left\langle \frac{1}{2},\mu_1',\frac{1}{2},\mu_2'\middle|s',m_s'\right\rangle\langle l',m_l',s',m_s'|j,\mu'''\rangle Y_{l'm_L'}(\hat{\mathbf{z}})D^{j}_{\mu'''\mu}(R) \\
&= \int d\hat{\mathbf{k}}''d\hat{\mathbf{k}}'\frac{1}{2j+1}\sum_{\mu''=-j}^{j}\left\langle \frac{1}{2},\mu_1,\frac{1}{2},\mu_2\middle|s,m_s\right\rangle\langle l,m_l,s,m_s|j,\mu''\rangle Y^*_{lm_l}[\hat{\mathbf{x}}\sin(\theta'')+\hat{\mathbf{z}}\cos(\theta'')] \\
&\quad\times\langle k''[\hat{\mathbf{x}}\sin(\theta'')+\hat{\mathbf{z}}\cos(\theta'')],\mu_1,\mu_2\|V\|k'\hat{\mathbf{z}},\mu_1',\mu_2'\rangle\left\langle \frac{1}{2},\mu_1',\frac{1}{2},\mu_2'\middle|s',m_s'\right\rangle\langle l',m_l',s',m_s'|j,\mu''\rangle Y_{l'm_l'}(\hat{\mathbf{z}}).
\end{aligned} \tag{B15}$$

Since all of the dependence on ϕ', θ', ϕ'' is in R, and the integrand is independent of R, these three angular integrals can be computed giving the multiplicative phase space factor of $8\pi^2$. What remains is the following integral over the cosine of the angle

between the final and initial momentum:

$$\langle k,l,s\|V^j\|k',l',s'\rangle = \int_{-1}^{1} du'' \frac{8\pi^2}{2j+1} \sum_{\mu''=-j}^{j} \left\langle \frac{1}{2},\mu_1,\frac{1}{2},\mu_2 \middle| s,m_s \right\rangle \langle l,m_l,s,m_s|j,\mu''\rangle Y^*_{lm_l}(\hat{\mathbf{x}}\sqrt{1-u''^2}+\hat{\mathbf{z}}u'') \times \langle k''(\hat{\mathbf{x}}\sqrt{1-u''^2}+\hat{\mathbf{z}}u''),\mu_1,\mu_2\|V\|k'\hat{\mathbf{z}}),\mu_1',\mu_2'\rangle \left\langle \frac{1}{2},\mu_1',\frac{1}{2},\mu_2' \middle| s',m_s' \right\rangle \langle l',m_l',s',m_s'|j,\mu''\rangle Y_{l'm_l'}(\hat{\mathbf{z}}). \tag{B16}$$

The last thing that needs for be addressed for an explicit formula is the spherical harmonics

$$Y^*_{lm}(\hat{\mathbf{x}}\sqrt{1-u''^2}+\hat{\mathbf{z}}u'') = (-)^{m_l}\sqrt{\frac{2l+1}{4\pi}}\sqrt{\frac{(l-m_l')!}{(l+m_l)!}}P_l^m(u'') = \sqrt{\frac{2l+1}{4\pi}}D^l_{m0}[R_y(\theta'')] \tag{B17}$$

$$Y_{l'm_l'}(\hat{\mathbf{z}}) = \delta_{m_l'0}\sqrt{\frac{2l'+1}{4\pi}}. \tag{B18}$$

Using these in the above expression we are left with a one-dimensional integral

$$\langle k,l,s\|V^j\|k',l',s'\rangle = \int_{-1}^{1} du'' \frac{8\pi^2}{2j+1} \sum_{\mu''=-j}^{j} \left\langle \frac{1}{2},\mu_1,\frac{1}{2},\mu_2 \middle| s,m_s \right\rangle \langle l,m_l,s,m_s|j,\mu''\rangle \sqrt{\frac{2l+1}{4\pi}} D^l_{m0}[R_y(\theta'')] \times \langle k''(\hat{\mathbf{x}}\sqrt{1-u''^2})+\hat{\mathbf{z}}u''),\mu_1,\mu_2\|V\|k'\hat{\mathbf{z}},\mu_1',\mu_2'\rangle \left\langle \frac{1}{2},\mu_1',\frac{1}{2},\mu_2' \middle| s',m_s' \right\rangle \langle l',0,s',m_s'|j,\mu''\rangle \sqrt{\frac{2l'+1}{4\pi}}. \tag{B19}$$

Cleaning this up gives the following expression for the partial wave amplitude:

$$\langle j,\mu,k,l,s|V|j',\mu',k',l',s'\rangle = \delta_{jj'}\delta_{\mu\mu'}\langle k,l,s\|V^j\|k',l',s'\rangle$$

with

$$\langle k,l,s\|V^j\|k',l',s'\rangle = \frac{8\pi^2}{2j+1}\sqrt{\frac{2l+1}{4\pi}}\sqrt{\frac{2l'+1}{4\pi}} \sum_{\mu''=-j}^{j} \sum \left\langle \frac{1}{2},\mu_1,\frac{1}{2},\mu_2 \middle| s,m_s \right\rangle \langle l,m_l,s,m_s|j\mu''\rangle \int_{-1}^{1} du'' D^l_{m0}[R_y(cos^{-1}(u'')] \times \langle k''(\hat{\mathbf{x}}\sqrt{1-u''^2})+\hat{\mathbf{z}}u''),\mu_1,\mu_2\|V\|k'\hat{\mathbf{z}},\mu_1',\mu_2'\rangle \left\langle \frac{1}{2},\mu_1',\frac{1}{2},\mu_2' \middle| s',m_s' \right\rangle \langle l',0,s',m_s'|j\mu''\rangle, \tag{B20}$$

where all repeated spin indices are summed. This reduces the partial-wave integral to a one-dimensional integral. In this case there are no traces, and no momentum-dependent spin bases, but there are a number of spin sums. Explicit computation requires

$$D^l_{m0}(R_y(\cos^{-1}(u'')) = \sum_{s=0}^{2j} \frac{\sqrt{j+m)!(j-m)!j!j!}}{(j+m-s)!s!(s-m)!(j-s)!} R_{11}^{j+m-s}R_{12}^{s}R_{21}^{s-m}R_{22}^{j+s} \tag{B21}$$

where all negative factorials are $^{\infty}$ and

$$R_{ij}[\cos^{-1}(u'')] = \begin{pmatrix} \sqrt{\frac{1+u''^2}{2}} & \sqrt{\frac{1-u''^2}{2}} \\ -\sqrt{\frac{1-u''^2}{2}} & \sqrt{\frac{1+u''^2}{2}} \end{pmatrix} \tag{B22}$$

or

$$D^l_{m0}(R_y(\cos^{-1}(u'')) = \sum_{s=0}^{2j} \frac{\sqrt{j+m)!(j-m)!j!j!}}{(j+m-s)!s!(s-m)!(j-s)!}(-1)^{s-m+0}\left(\sqrt{\frac{1+u''^2}{2}}\right)^{2j+m}\left(\sqrt{\frac{1-u''^2}{2}}\right)^{2s-m}. \tag{B23}$$

APPENDIX C

The electromagnetic corrections to the nucleon-nucleon interaction have the following forms for the pp, np, and nn systems:

$$V_{\mathrm{em\,pp}}(r) = [v_{\mathrm{em},1}(r)+v_{\mathrm{em},2}(r)+v_{\mathrm{em},3}(r)+v_{\mathrm{em},4}(r)]I + v_{\mathrm{em},6}(r)\boldsymbol{\sigma}_1\cdot\boldsymbol{\sigma}_2 + v_{\mathrm{em},9}(r)S_{12} + v_{\mathrm{em},12}(r)\mathbf{L}\cdot\mathbf{S} \tag{C1}$$

$$V_{\mathrm{em\,np}}(r) = v_{\mathrm{em},5}(r)I + v_{\mathrm{em},8}(r)\boldsymbol{\sigma}_1\cdot\boldsymbol{\sigma}_2 + v_{\mathrm{em},11}(r)S_{12} + v_{\mathrm{em},14}(r)\mathbf{L}\cdot\mathbf{S} \tag{C2}$$

$$V_{\mathrm{em\,nn}}(r) = v_{\mathrm{em},7}(r)\boldsymbol{\sigma}_1\cdot\boldsymbol{\sigma}_2 + v_{\mathrm{em},10}(r)S_{12} + v_{\mathrm{em},13}(r)\mathbf{L}\cdot\mathbf{S} \tag{C3}$$

The Fourier transforms have the same structure as they do for the strong interactions.

$$\tilde{V}_{\mathrm{em\,pp}}(q) = [v_{\mathrm{em},1}(q) + v_{\mathrm{em},2}(q) + v_{\mathrm{em},3}(q) + v_{\mathrm{em},4}(q)]I + v_{\mathrm{em},6}(q)\boldsymbol{\sigma}_1\cdot\boldsymbol{\sigma}_2 + v_{\mathrm{em},9}(q)\tilde{S}_{12} + i\,v_{\mathrm{em},12}(q)(\mathbf{k}\times\mathbf{k}')\cdot\mathbf{S}. \quad \text{(C4)}$$

$$\tilde{V}_{\mathrm{em\,np}}(q) = v_{\mathrm{em},5}(q)I + v_{\mathrm{em},8}(q)\boldsymbol{\sigma}_1\cdot\boldsymbol{\sigma}_2 + v_{\mathrm{em},11}(q)\tilde{S}_{12} + i\,v_{\mathrm{em},14}(q)(\mathbf{k}\times\mathbf{k}')\cdot\mathbf{S}. \quad \text{(C5)}$$

$$\tilde{V}_{\mathrm{em\,nn}}(q) = v_{\mathrm{em},7}(q)\boldsymbol{\sigma}_1\cdot\boldsymbol{\sigma}_2 + v_{\mathrm{em},10}(q)\tilde{S}_{12} + i\,v_{\mathrm{em},13}(q)(\mathbf{k}\times\mathbf{k}')\cdot\mathbf{S}. \quad \text{(C6)}$$

where

$$\tilde{S}_{12} := -3[(\mathbf{q}\cdot\boldsymbol{\sigma}_1)(\mathbf{q}\cdot\boldsymbol{\sigma}_2) - \boldsymbol{\sigma}_1\cdot\boldsymbol{\sigma}_2]. \quad \text{(C7)}$$

The coefficients of I, $\boldsymbol{\sigma}_1\cdot\boldsymbol{\sigma}_2$ are

$$\tilde{v}_{\mathrm{em,n}}(q) = \frac{1}{2\pi^2}\int_0^\infty j_0(qr)v_{\mathrm{em,n}}(r)r^2dr \quad \times n \in \{1,2,3,4,5,6,7,8\}; \quad \text{(C8)}$$

the coefficients of $i(\mathbf{k}\times\mathbf{k}')\cdot\mathbf{S}$ are

$$\tilde{v}_{\mathrm{em,n}}(q) = \frac{1}{2\pi^2 q}\int_0^\infty j_1(qr)v_{\mathrm{em,n}}(r)r^3dr \quad n \in \{12,13,14\} \quad \text{(C9)}$$

and the coefficients of $\tilde{S}_{12}$, are

$$\tilde{v}_{\mathrm{em,n}}(q) = \frac{1}{2\pi^2 q^2}\int_0^\infty j_2(qr)v_{\mathrm{em,n}}(r)r^2dr \quad n \in \{9,10,11\} \quad \text{(C10)}$$

where the individual terms are

$$v_{\mathrm{em},1}(r) = \frac{\alpha\hbar c}{r}\left\{1 - \left[1 + \frac{11}{16}br + \frac{3}{16}(br)^2 + \frac{1}{48}(br)^3\right]e^{-br}\right\}, \quad \text{(C11)}$$

$$v_{\mathrm{em},2}(r) = -\frac{\alpha(\hbar c)^3}{4m_p^2}\frac{b^3}{16}\left[1 + br + \frac{1}{3}(br)^2\right]e^{-br}, \quad \text{(C12)}$$

$$v_{\mathrm{em},3}(r) = -\frac{1}{m_p}v_{\mathrm{em}}(1)^2, \quad \text{(C13)}$$

$$v_{\mathrm{em},4}(r) = \frac{2\alpha}{3\pi}\left(-\gamma - \frac{5}{6} + |\ln(ar)|\right)v_{\mathrm{em},1}(r), \quad \text{(C14)}$$

$$v_{\mathrm{em},5}(r) = \alpha\hbar c\beta\frac{b^3}{384}[15 + 15br + 6(br)^2 + (br)^3]e^{-br}, \quad \text{(C15)}$$

$$v_{\mathrm{em},6}(r) = -\frac{\alpha(\hbar c)^3\mu_p^2}{6m_p^2}\frac{b^3}{16}\left[1 + br + \frac{1}{3}(br)^2\right]e^{-br}, \quad \text{(C16)}$$

$$v_{\mathrm{em},7}(r) = -\frac{\alpha(\hbar c)^3\mu_n^2}{6m_n^2}\frac{b^3}{16}\left[1 + br + \frac{1}{3}(br)^2\right]e^{-br}, \quad \text{(C17)}$$

$$v_{\mathrm{em},8}(r) = -\frac{\alpha(\hbar c)^3\mu_n\mu_p}{6m_nm_p}\frac{b^3}{16}\left[1 + br + \frac{1}{3}(br)^2\right]e^{-br}, \quad \text{(C18)}$$

$$v_{\mathrm{em},9}(r) = -\frac{\alpha(\hbar c)^3\mu_p^2}{4m_p^2}\frac{1}{r^3}\left\{1 - \left[1 + br + \frac{1}{2}(br)^2 + \frac{1}{6}(br)^3 + \frac{1}{24}(br)^4 + \frac{1}{144}(br)^5\right]e^{-br}\right\}, \quad \text{(C19)}$$

$$v_{\mathrm{em},10}(r) = -\frac{\alpha(\hbar c)^3\mu_n^2}{4m_n^2}\frac{1}{r^3}\left\{1 - \left[1 + br + \frac{1}{2}(br)^2 + \frac{1}{6}(br)^3 + \frac{1}{24}(br)^4 + \frac{1}{144}(br)^5\right]e^{-br}\right\}, \quad \text{(C20)}$$

$$v_{\mathrm{em},11}(r) = -\frac{\alpha(\hbar c)^3\mu_p\mu_n}{4m_pm_n}\frac{1}{r^3}\left\{1 - \left[1 + br + \frac{1}{2}(br)^2 + \frac{1}{6}(br)^3 + \frac{1}{24}(br)^4 + \frac{1}{144}(br)^5\right]e^{-br}\right\}, \quad \text{(C21)}$$

$$v_{\mathrm{em},12}(r) = -\frac{\alpha(\hbar c)^3(4\mu_p - 1)\mu_p\mu_n}{2m_p^2}\frac{1}{r^3}\left\{1 - \left[1 + br + \frac{1}{2}(br)^2 + \frac{7}{48}(br)^3\right]e^{-br}\right\}, \quad \text{(C22)}$$

$$v_{\mathrm{em},13}(r) = 0, \quad \text{(C23)}$$

and

$$v_{\mathrm{em},14}(r) = -\frac{\alpha(\hbar c)^3\mu_n}{2m_nm_r}\frac{1}{r^3}\left\{1 - \left[1 + br + \frac{1}{2}(br)^2 + \frac{7}{48}(br)^3\right]e^{-br}\right\}, \quad \text{(C24)}$$

where $b = 4.27$ and $a = m_e/(\hbar c)$, $\mu_p = 2.7928474$, and $\mu_n = -1.9130427$, $\beta = .0189$.

The Fourier transform of most of the terms in the potential can be computed using direct integration, the identities

$$j_1(x) = -\frac{d}{dx}j_0(x) \qquad \frac{1}{x}j_2(x) = -\frac{d}{dx}\frac{j_1(x)}{x}, \quad \text{(C25)}$$

and the following relation [13], with $\nu = l + \frac{1}{2}$ and $\mu = n + 1/2$, gives the relation

$$\int_0^\infty e^{-br}j_l(qr)r^n dx = \frac{q^l}{b^{n+l+1}}\frac{(n+l)!}{(2l+1)!!} \times F\left(\frac{n+l+1}{2}, \frac{n+l+2}{2}, \frac{2l+3}{2}, -q^2/b^2\right), \quad \text{(C26)}$$

which is valid for $n + l > -1$.

The only integral that cannot be computed using these formulas involves the $|\ln(kr)|$ term that appears in $v_{\mathrm{em}\,4}(r)$, which is an approximation to the vacuum polarization correction to the pp interaction. The required integrals, which are evaluated in this appendix are

$$\int_0^\infty j_0(qr)|\ln(ar)|rdr = \frac{a^2}{q}[\gamma + 3\ln(q/a) - 2\mathrm{ci}(q/a)], \tag{C27}$$

$$\begin{aligned}\int_0^\infty & j_0(qr)|\ln(ar)|re^{-br}dr \\ &= \frac{a^3}{b^2+q^2}\left[b\tan^{-1}\left(\frac{q}{b}\right) - q\gamma + \frac{q}{2}\ln(q^2/a^2 + b^2/a^2)\right] \\ &\quad + \frac{a^3}{q^2+b^2}\left[q\frac{\left[E_1\left(\frac{b-iq}{a}\right) + E_1\left(\frac{b+iq}{a}\right)\right]}{2}\right. \\ &\quad \left. + b\frac{\left[E_1\left(\frac{b-iq}{a}\right) - E_1\left(\frac{b+iq}{a}\right)\right]}{2i}\right],\end{aligned} \tag{C28}$$

$$\begin{aligned}\int_0^\infty & j_0(qr)|\ln(ar)|r^2e^{-br}dr \\ &= -\frac{\partial}{\partial b}\int_0^\infty j_0(qr)|\ln(ar)|re^{-br}dr,\end{aligned} \tag{C29}$$

$$\begin{aligned}\int_0^\infty & j_0(qr)|\ln(ar)|r^3e^{-br}dr \\ &= \frac{\partial^2}{\partial b^2}\int_0^\infty j_0(qr)|\ln(ar)|re^{-br}dr,\end{aligned} \tag{C30}$$

$$\begin{aligned}\int_0^\infty & j_0(qr)|\ln(ar)|r^4e^{-br}dr \\ &= -\frac{\partial^3}{\partial b^3}\int_0^\infty j_0(qr)|\ln(ar)|re^{-br}dr,\end{aligned} \tag{C31}$$

and

$$\int_0^\infty j_2(qr)r^{-1}dr = \lim_{x\to 0} j_1(x)/x = 1/3. \tag{C32}$$

The vacuum polarization integral only appears in the Coulomb potential, which has the approximate form given in Ref. [14]—this approximation is adequate for binding energy calculations. It appears in the following contribution to the proton-proton interaction:

$$\begin{aligned}v_{\mathrm{em}(4)}(r) = \frac{2\alpha}{3\pi}&\left(-\gamma - \frac{5}{6} + |\ln(ar)| + \frac{6\pi kr}{8}\right)\frac{\alpha\hbar c}{r} \\ &\times (1 - e^{-br}\left(1 + \frac{11}{16}br + \frac{3}{16}(br)^2 + \frac{1}{48}(br)^3\right).\end{aligned} \tag{C33}$$

The Fourier Bessel transform of this interaction,

$$\begin{aligned}\frac{1}{2\pi^2 q}&\int_0^\infty j_0(qr)V_{\mathrm{em}(4)}(r)r^2dr \\ &= \frac{1}{2\pi^2q^2}\int_0^\infty \sin(qr)\frac{2\alpha}{3\pi}\left(-\gamma - \frac{5}{6} + |\ln(ar)| + \frac{6\pi kr}{8}\right)\alpha\hbar c(1 - e^{-br}\left(1 + \frac{11}{16}br + \frac{3}{16}(br)^2 + \frac{1}{48}(br)^3\right), dr\end{aligned} \tag{C34}$$

can be computed analytically. There are three types of contributions

$$(i) = \frac{1}{2\pi^2q^2}\int_0^\infty \sin(qr)\frac{2\alpha}{3\pi}\left(-\gamma - \frac{5}{6}\right)\alpha\hbar c(1 - e^{-br}\left(1 + \frac{11}{16}br + \frac{3}{16}(br)^2 + \frac{1}{48}(br)^3\right)dr, \tag{C35}$$

$$(ii) = \frac{1}{2\pi^2q^2}\int_0^\infty \sin(qr)\frac{2\alpha}{3\pi}|\ln(ar)|\alpha\hbar c(1 - e^{-br}\left(1 + \frac{11}{16}br + \frac{3}{16}(br)^2 + \frac{1}{48}(br)^3\right), dr, \tag{C36}$$

and

$$(iii) = \frac{1}{2\pi^2q^2}\int_0^\infty \sin(qr)\frac{2\alpha}{3\pi}\frac{6\pi kr}{8}\alpha\hbar c(1 - e^{-br}\left(1 + \frac{11}{16}br + \frac{3}{16}(br)^2 + \frac{1}{48}(br)^3\right)dr. \tag{C37}$$

Integrals of the form (i) and (iii) have the same form as the integrals discussed above. To calculate the integral (ii) first replace $r' = ar \to r = r'/a$ to get

$$\begin{aligned}(ii) &= \frac{1}{2a\pi^2q^2}\int_0^\infty \sin(qr'/a)\frac{2\alpha}{3\pi}|\ln(r')|\alpha\hbar c\left(1 - e^{-br'/a}\left(1 + \frac{11}{16}\frac{br'}{a} + \frac{3}{16}\left(\frac{br'}{a}\right)^2 + \frac{1}{48}\left(\frac{br'}{a}\right)^3\right)\right)dr' \\ &= \frac{1}{2a\pi^2q^2}\frac{2\alpha}{3\pi}\alpha\hbar c\int_0^\infty \sin(qr'/a)|\ln(r')|dr' - \frac{1}{2a\pi^2q^2}\frac{2\alpha}{3\pi}\alpha\hbar c\left(1 + \frac{11}{16}\left(-b\frac{d}{db}\right) + \frac{3}{16}\left(b^2\frac{d^2}{d^2b}\right)\right. \\ &\quad \left. + \frac{1}{48}\left(-b^3\frac{d^3}{d^3b}\right)\right)\int_0^\infty \sin(qr'/a)e^{-br'/a}|\ln(r')|dr'.\end{aligned} \tag{C38}$$

Two integrals need to be performed to compute this term. They are

$$\int_0^\infty \sin(qr'/a)|\ln(r')|dr' \tag{C39}$$

and

$$\int_0^\infty \sin(qr'/a)e^{-br'/a}|\ln(r')|dr'. \tag{C40}$$

The integral

$$\int_0^\infty \sin(qr'/a)|\ln(r')|dr' = -\int_0^1 \sin(qr'/a)\ln(r')dr' + \lim_{d\to 0}\left[\int_0^\infty \sin(qr'/a)e^{-dr'}\ln(r')dr' - \int_0^1 \sin(qr'/a)\ln(r')dr'\right]. \tag{C41}$$

These integrals can be found in Ref. [15]

$$\int_0^1 \sin(qx)\ln(x)dx = -\frac{1}{q}[\gamma + \ln(q) - \mathrm{ci}(q)] \tag{C42}$$

where

$$\mathrm{ci}(x) = \mathrm{Ci}(x) = -\int_x^\infty \frac{\cos(t)}{t} \tag{C43}$$

and

$$\int_0^\infty e^{-br}\sin(qr)\ln(r)dr = \frac{1}{b^2+q^2}\left[b\tan^{-1}\left(\frac{q}{b}\right) - q\gamma + \frac{q}{2}\ln(q^2+b^2)\right]. \tag{C44}$$

The quantity γ is the Euler constant. Thus the first of the required integrals needed to compute the vacuum polarization contribution is

$$\begin{aligned}\int_0^\infty |\ln(r')|\sin(qr'/a)dr' &= -\int_0^1 \sin(qr'/a)\ln(r')dr' + \lim_{d\to 0}\left[\int_0^\infty e^{-dr'}\sin(qr'/a)\ln(r')dr' - \int_0^1 \ln(r')\sin(qr'/a)\right] \\ &= -2\int_0^1 \ln(r')\sin(qr'/a)dr' + \lim_{d\to 0}\int_0^\infty e^{-dr'}\sin(qr'/a)\ln(r')dr' = \frac{2a}{q}[\gamma + \ln(q/a) - \mathrm{ci}(q/a)] \\ &\quad + \frac{a}{q}\left[-\gamma + \frac{1}{2}\ln(q^2/a^2)\right] = \frac{a}{q}[\gamma + 3\ln(q/a) - 2\mathrm{ci}(q/a)].\end{aligned} \tag{C45}$$

Returning to the original expression, the first term in (ii) is

$$\frac{1}{2a\pi^2q^2}\frac{2\alpha}{3\pi}\alpha\hbar c\int_0^\infty \sin(qr'/a)|\ln(r')|dr' = \frac{\alpha^2\hbar c}{3\pi^3q^3}[\gamma + 3\ln(q/a) - 2\mathrm{ci}(q/a)] \tag{C46}$$

where γ is the Euler constant. Or

$$\frac{1}{2\pi^2q^2}\int_0^\infty \sin(qr)\frac{2\alpha}{3\pi}|\ln(ar)|\alpha\hbar c = \frac{\alpha^2\hbar c}{3\pi^3q^3}[\gamma + 3\ln(q/a) - 2\mathrm{ci}(q/a)]. \tag{C47}$$

We also have to compute the second term in (ii). The integral that is needed is

$$-\frac{\alpha^2\hbar c}{3\pi^3aq^2}\int_0^\infty \sin(qr'/a)|\ln(r')|e^{-br'/a}\left(1 + \frac{11}{16}\frac{br'}{a} + \frac{3}{16}\left(\frac{br'}{a}\right)^2 + \frac{1}{48}\left(\frac{br'}{a}\right)^3\right)dr'. \tag{C48}$$

This can be evaluated using

$$-\int_0^\infty \sin(qr'/a)|\ln(r')|e^{-br'/a}dr' = \int_0^\infty \sin(qr'/a)\ln(r')e^{-br'/a}dr' - 2\int_1^\infty \sin(qr'/a)\ln(r')e^{-br'/a}dr' \tag{C49}$$

by differentiation with respect to b. The integral

$$\begin{aligned}\int_1^\infty \sin(qr'/a)\ln(r')e^{-br'/a}dr' &= \frac{1}{2i}\int_1^\infty (e^{(iq/a-b/a)r'} - e^{(-iq/a-b/a)r'})\ln(r')dr' = -\frac{a}{2i}\int_1^\infty \frac{dr'}{r'}\left[\frac{e^{(iq/a-b/a)r'}}{iq-b} + \frac{e^{(-iq/a-b/a)r'}}{iq+b}\right] \\ &\quad - \frac{a}{2i}\left[\frac{E_1\left(\frac{b-iq}{a}\right)}{iq-b} + \frac{E_1\left(\frac{b+iq}{a}\right)}{iq+b}\right]\frac{a}{2i(q^2+b^2)}\left[(iq+b)E_1\left(\frac{b-iq}{a}\right) + (iq-b)E_1\left(\frac{b+iq}{a}\right)\right] \\ &= \frac{a}{q^2+b^2}\left[q\frac{\left(E_1\left(\frac{b-iq}{a}\right) + E_1\left(\frac{b+iq}{a}\right)\right)}{2} + b\frac{\left(E_1\left(\frac{b-iq}{a}\right) - E_1\left(\frac{b+iq}{a}\right)\right)}{2i}\right].\end{aligned} \tag{C50}$$

Thus

$$\int_1^\infty \sin(qr'/a)\ln(r')e^{-br'/a}dr' = \frac{a}{q^2+b^2}\left[q\frac{\left(E_1\left(\frac{b-iq}{a}\right)+E_1\left(\frac{b+iq}{a}\right)\right)}{2}+b\frac{\left(E_1\left(\frac{b-iq}{a}\right)-E_1\left(\frac{b+iq}{a}\right)\right)}{2i}\right]. \tag{C51}$$

Combining the two integrals gives

$$-\frac{\alpha^2\hbar c}{3\pi^3 aq^2}\int_0^\infty \sin(qr'/a)|\ln(r')|e^{-br'/a}dr' = -\frac{\alpha^2\hbar c}{3\pi^3 aq^2}\times\left\{\frac{a}{b^2+q^2}\left[b\tan^{-1}\left(\frac{q}{b}\right)-q\gamma+\frac{q}{2}\ln(q^2/a^2+b^2/a^2)\right]\right.$$
$$\left.+\frac{a}{q^2+b^2}\left[q\frac{\left(E_1\left(\frac{b-iq}{a}\right)+E_1\left(\frac{b+iq}{a}\right)\right)}{2}+b\frac{\left(E_1\left(\frac{b-iq}{a}\right)-E_1\left(\frac{b+iq}{a}\right)\right)}{2i}\right]\right\}. \tag{C52}$$

Putting all of the parts together gives the $\ln(r)$ contribution to the vacuum polarization contribution

$$(ii)_b = \frac{\alpha^2\hbar c}{3\pi^3 q^3}[\gamma+3\ln(q/a)-2\mathrm{ci}(q/a)]+-\left(1+\frac{11}{16}\left(-b\frac{d}{db}\right)+\frac{3}{16}\left(b^2\frac{d^2}{db^2}\right)+\frac{1}{48}\left(-b^3\frac{d^3}{db^3}\right)\right)$$
$$\times\frac{\alpha^2\hbar c}{3\pi^3 aq^2}\left\{\frac{a}{b^2+q^2}\left[b\tan^{-1}\left(\frac{q}{b}\right)-q\gamma+\frac{q}{2}\ln(q^2/a^2+b^2/a^2)\right]\right.$$
$$\left.+\frac{a}{q^2+b^2}\left[q\frac{\left(E_1\left(\frac{b-iq}{a}\right)+E_1\left(\frac{b+iq}{a}\right)\right)}{2}+b\frac{\left(E_1\left(\frac{b-iq}{a}\right)-E_1\left(\frac{b+iq}{a}\right)\right)}{2i}\right]\right\}. \tag{C53}$$

This needs to be added to (i) and (ii) to get the full vacuum polarization integral. These integrals can be computed using the methods used for all of the other potentials. The exponential integrals have simple derivatives

$$\frac{d}{dx}E_1(x) = -\frac{e^{-x}}{x}. \tag{C54}$$

[1] R. B. Wiringa, V. G. J. Stoks, and R. Schiavilla, Phys. Rev. C **51**, 38 (1995).

[2] V. G. J. Stoks, R. A. M. Klomp, C. P. F. Terheggen, and J. J. de Swart, Phys. Rev. C **49**, 2950 (1994).

[3] R. Machleidt, Phys. Rev. C **63**, 024001 (2001).

[4] W. Glöckle, H. Witala, D. Hüber, H. Kamada, and J. Golak, Phys. Rep. **274**, 107 (1986).

[5] S. Veerasamy, Ph.D. thesis, University of Iowa, 2011 (unpublished).

[6] R. Broucke, Communications of the Association for Computing Machinery, 16 (1973), p. 254.

[7] See Supplemental Material at http://link.aps.org/supplemental/10.1103/PhysRevC.84.034003 for argonne_chebyshev.c.

[8] B. D. Keister and W. N. Polyzou, J. Comput. Phys. **134**, 231 (1997).

[9] See Supplemental Material at http://link.aps.org/supplemental/10.1103/PhysRevC.84.034003 for argonne_rational.c.

[10] J. Golak, W. Glöckle, R. Skibiński, H. Witała, D. Rozpkedzik, K. Topolnicki, I. Fachruddin, Ch. Elster, and A. Nogga, Phys. Rev. C **81**, 034006 (2010).

[11] Robert Wiringa (private communication).

[12] J. Golak *et al.*, arXiv:0911.4173.

[13] I. S. Gradshteyn and I. M. Ryzhik, *Tables of Integrals, Series, and Products* (Academic Press, San Diego, 1994), p. 711, Eq. 6.621.

[14] N. Auerbach, J. Hüfner, A. K. Kerman, and C. M. Shakin, Rev. Mod. Phys. **44**, 48 (1972).

[15] I. S. Gradshteyn and I. M. Ryzhik, *Tables of Integrals, Series, and Products* (Academic Press, San Diego, 1994), p. 583, Eq. 4.381; p. 605, Eq. 4.441.